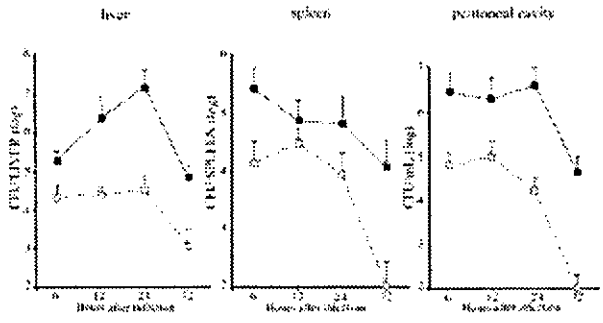

Fig. 2. Delayed clearance of *E. coli* in liver, spleen, and peritoneal cavity in BDL mice. Data are representative of 4 separate experiments and are expressed as the mean ± SD for 5 mice in an experiment. (■) BDL mice. (□) Sham-operated mice. CFU, colony-forming units.

at 6 hours after *E. coli* infection when a large difference in number of viable bacteria was seen (Fig. 3). The numbers of polymorphonuclear cells and macrophages were significantly larger at 24 hours in BDL mice after *E. coli* infection, presumably due to increased bacterial burden at this stage. These results indicate that accumulation of phagocytes is not impaired in BDL mice after *E. coli* infection.

***Aberrant Cytokine Production in BDL Mice After* E. coli *Challenge.*** Cytokine production was examined in the sera of sham-operated and BDL mice after *E. coli* infection. As shown in Fig. 4A, serum TNF-α and IL-10 levels were maximal at 1 hour after *E. coli* infection, while the IL-12 level reached a peak at 3 hours after infection in both BDL and sham-operated mice. Serum IL-10 levels were significantly higher in BDL mice than in sham-operated mice, while increases in IL-12 levels were significantly suppressed in BDL mice ($P < .05$). There was no significant difference in serum TNF-α level between sham-operated and BDL mice. The patterns of cytokine profile of peritoneal lavage fluid were similar to those of the serum (Fig. 4B). Neither IL-4 nor IFN-γ was detected in the sera or peritoneal lavage fluids of either BDL or sham-operated mice at any stage after *E. coli* infection (data not shown). These results clearly indicated that mice with obstructive jaundice present predominant IL-10 production over IL-12 after *E. coli* infection.

***IFN-γ Production By Liver Lymphocytes of BDL Mice After* E. coli *Infection.*** To further investigate the cytokine profiles in BDL mice, we next examined messenger RNA (mRNA) expression in the whole liver homogenates of BDL mice or sham-operated mice after *E. coli* infection. Consistent with serum cytokine levels, high expression of IL-10 mRNA together with low expression of IL-12p40 mRNA was seen in BDL mice. Notably, expression of IFN-γ mRNA was not increased in liver of BDL mice after *E. coli* infection (Fig. 5A).

Because IFN-γ is necessary for macrophages to be activated so that they may kill microorganisms, we next determine the quantitative difference in IFN-γ production by liver lymphocytes between BDL and sham-operated mice. The expression of IFN-γ mRNA remained suppressed in liver lymphocytes isolated from BDL mice at any time point after *E. coli* infection compared with those from sham-operated mice (Fig. 5B). Moreover, whereas liver lymphocytes isolated from sham-operated mice 6 hours after *E. coli* infection produced a high level of IFN-γ *in vitro* without additional stimulation, IFN-γ production was barely detectable in lymphocytes from BDL mice (Fig. 5C).

***Differences in Cytokine Production Between Kupffer Cells and Peritoneal Macrophages of BDL Mice.*** To seek the source of serum cytokines produced after *E. coli* inoculation, we compared cytokine production by Kupffer cells with that by peritoneal macrophages in response to LPS derived from *E. coli* in vitro. The peritoneal macrophages and Kupffer cells isolated from BDL or sham-operated mice were stimulated *in vitro* with LPS, and the concentrations of TNF-α, IL-12, and IL-10 in the culture supernatants were determined via ELISA. As shown in Fig. 6A, the peritoneal macrophages of BDL mice produced considerably higher levels of TNF-α but significantly lower levels of IL-10 3 hours after LPS stimulation than those of sham-operated mice. The level of IL-12p40 production was higher in the peritoneal macrophages of BDL mice at 10 hours and 16 hours after LPS stimulation compared with those of sham-operated mice.

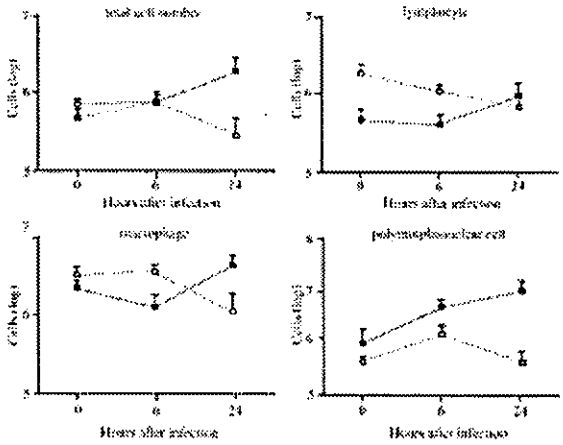

Fig. 3. Kinetics of peritoneal exudate cells of sham-operated (□) and BDL (■) mice after intraperitoneal inoculation with $10^7$ colony-forming units of *E. coli* were analyzed with flow cytometry. Accumulation of immune cells after *E. coli* infection was not impaired in BDL mice. Data are representative of 3 separate experiments and are expressed as the mean ± SD for 4 mice in an experiment.

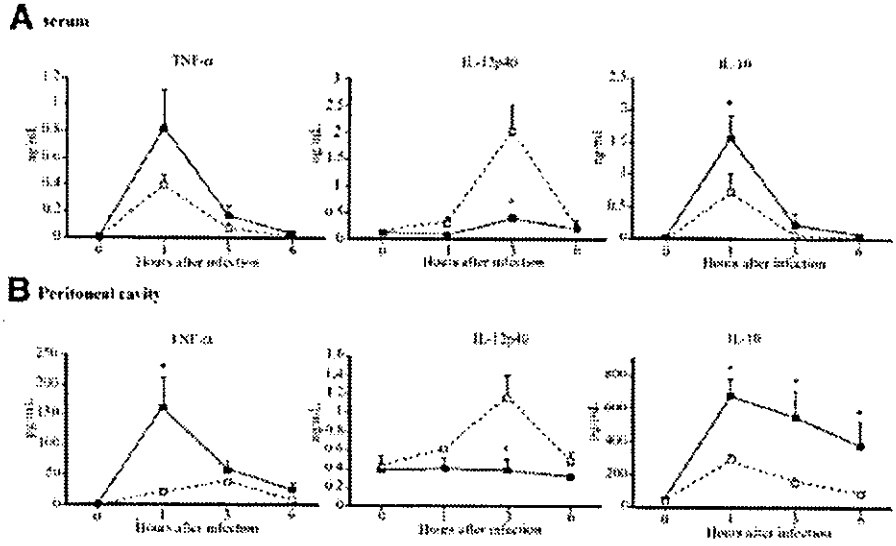

Fig. 4. Kinetics of cytokine levels in (A) serum and (B) peritoneal lavage fluid after *E. coli* challenge. Plasma and peritoneal lavage fluid samples were obtained at the indicated time points after intraperitoneal inoculation with $10^7$ colony-forming units of *E. coli*. TNF-α, IL-12, and IL-10 concentrations were determined via EUSA. Data are representative of 3 separate experiments and are expressed as the mean ± SD for 5 mice in an experiment. $^*P < .05$ versus the sham-operated group. (■) BDL mice. (□) Sham-operated mice. TNF-α, tumor necrosis factor α; IL, interleukin.

On the other hand, Kupffer cells from BDL mice, in response to LPS, produced a larger amount of IL-10 and a smaller amount of IL-12 compared with those from sham-operated mice (Fig. 6B). There was no difference in TNF-α production by Kupffer cells between BDL and sham-operated mice.

We further compared mRNA expression for IL-10, IL-12p40, and TNF-α in Kupffer cells and peritoneal macrophages between BDL and sham-operated mice after LPS stimulation. As shown in Fig. 5D and 5E, IL-10 mRNA was increased in Kupffer cells of BDL mice after LPS stimulation, whereas the peritoneal macrophages of BDL mice expressed less IL-10 mRNA than those of sham-operated mice. Increase in IL-12p40 mRNA was only marginal in Kupffer cells of BDL mice but prominent in the peritoneal macrophages of BDL mice after LPS stimulation. TNF-α mRNA increased more markedly in both Kupffer cells and peritoneal macrophages of BDL mice after LPS stimulation compared with those in sham-operated mice. These results indicate that peritoneal macrophages and Kupffer cells from BDL mice respond differently to LPS in terms of IL-10 and IL-12 production and that the cytokine profiles of peritoneal macrophages are similar to those of Kupffer cells in sham-operated mice.

***Effect of IL-10 Neutralization on Resolution of* E. coli *Infection.*** Because IL-10 is known to hamper the resolution of bacterial infection in mice, we next determined whether or not increased IL-10 production in BDL mice is responsible for the impaired host defense against *E. coli* infection. BDL mice were injected intraperitoneally with anti–IL-10 neutralizing mAb (200 μg/mouse) 2 hours before *E. coli* challenge, and the number of the bacteria in organs was examined 24 hours after infection. As shown in Fig. 7, impaired bactericidal activity was reversed by administration of anti–IL-10 mAb in BDL mice. These results suggest that early IL-10 production by Kupffer cells might be responsible for hampered resolution of *E. coli* infection in BDL mice.

***IL-10 Production in Fas-Mutated BDL Mice After* E. coli *Infection.*** As demonstrated above, we found that BDL induced predominant IL-10 production specifically by Kupffer cells in mice. We hypothesized that Kupffer cells in BDL mice have been changed to readily produce IL-10 as a result of ingesting apoptotic hepatocytes, because it is demonstrated that macrophages produce IL-10 after ingesting apoptotic cells to prevent unnecessary immune responses.[16,17] To investigate this possibility, Fas-mutated *lpr/lpr* (*lpr*) mice were used in the next experiment, because *lpr* mice are shown to be resistant to cholestatic liver injury, which partially involves Fas-dependent hepatocyte apoptosis. As shown in Fig. 1E, hepatocyte apoptosis was seen in liver of BDL mice, whereas few apoptotic hepatocytes were observed in liver of *lpr* mice undergoing BDL (Fig. 1F); this is consistent with previous reports.[19,29] There was no difference in serum total bilirubin levels between wild type and *lpr* mice after BDL, but serum alanine aminotransferase activity of *lpr* mice was significantly lower in *lpr* mice than in wild type mice (42.2 ± 12.4 IU/L vs. 85.1 ± 15.6 IU/L; $P < .05$). As expected, serum IL-10 level of BDL-*lpr* mice after *E. coli* infection was comparable to that of sham-operated mice (Fig. 8B). Surprisingly, the bacterial number in organs 24 hours after *E. coli* infection was significantly lower in BDL-*lpr* mice when compared with BDL wild type mice, whereas no significant difference in bacterial clear-

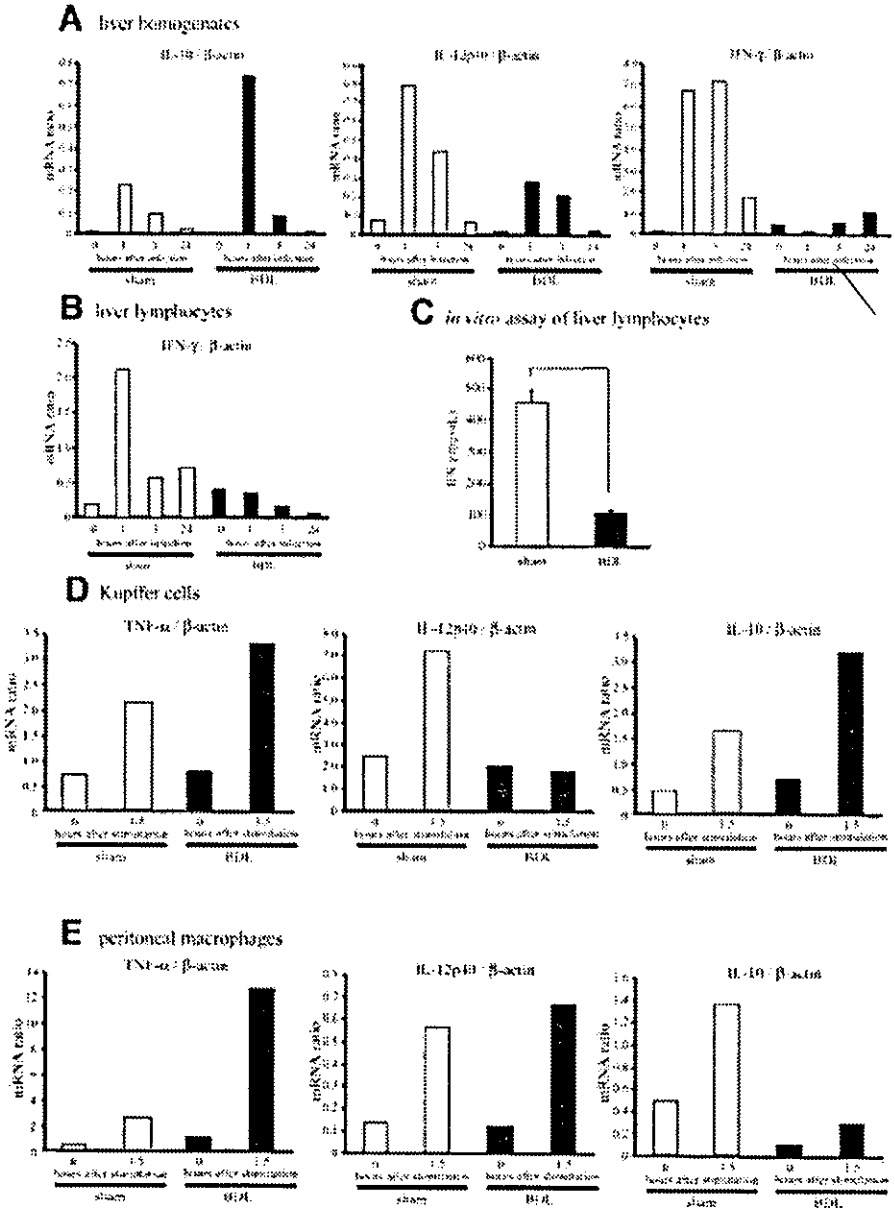


Fig. 5. Cytokine gene expressions in (A) liver homogenates and (B) liver lymphocytes after *E. coli* infection and in (D) Kupffer cells and (E) peritoneal macrophages after LPS stimulation. Cytokine gene expressions were quantitated using real-time polymerase chain reaction. Cytokine mRNA expressions of liver homogenates and liver lymphocytes were pooled from 4 mice in each group after *E. coli* infection. Cytokine gene expressions of cultured Kupffer cells and peritoneal macrophages were pooled from 5 mice in each group before and after stimulation with LPS (0.1 μg/mL). The expression of mRNA levels for each cytokines were normalized as a ratio using β-actin mRNA as a housekeeping gene. (C) *In vitro* IFN-γ production of liver lymphocytes after *E. coli* infection in sham-operated and BDL mice. Liver lymphocytes were isolated from each group before and after *E. coli* infection and cultured *in vitro* for 24 hours without additional stimulation. Culture supematants were analyzed for IFN-γ content via ELISA. IFN-γ was not detected in culture supematants of sham-operated or BDL mice before infection. Results were derived from 6-8 mice per group. $^*P < .05$. IL, interleukin; IFN-γ, interferon γ; mRNA, messenger RNA; BDL, bile duct ligation; TNF-α, tumor necrosis factor α;

ance was seen between sham and sham-*lpr* mice (Fig. 8A). These results indicate that Fas may be partially involved in increased IL-10 production by Kupffer cells and subsequent impairment in bacterial killing in BDL mice.

## Discussion

Although bile duct ligation has been shown to induce impairment in bacterial clearance, only a few reports have addressed the bactericidal activity in cholestatic animals from a standpoint of pro- and anti-inflammatory cytokines.[27,28] We show here that increased IL-10 production with decreased IL-12 release in the serum following *E. coli* infection is characteristic of BDL mice as opposed to sham-operated mice. The early IL-10 production was potentially involved in impaired resolution of *E. coli* infection because *in vivo* administration of anti–IL-10 mAb significantly augmented bacterial clearance in BDL mice. We concluded that Kupffer cells were major sources of serum cytokines because these serum cytokine levels were well correlated with those produced by Kupffer cells but not peritoneal macrophages.

T cells and natural killer cells, in the presence of IL-12, initially produce IFN-γ after bacterial infection; later increase in IL-10 suppresses IFN-γ production by these

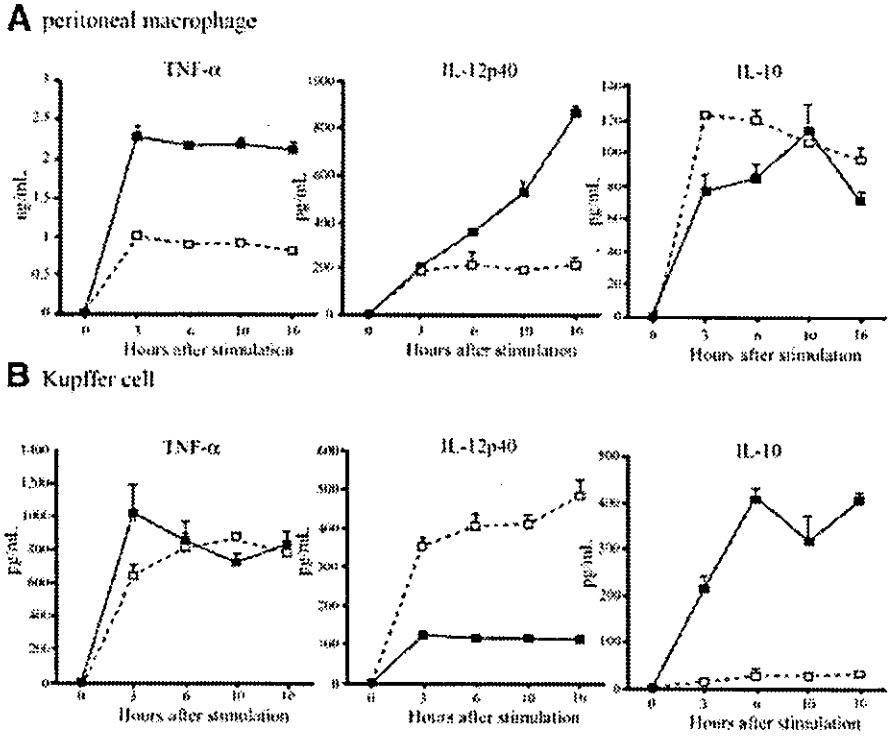


Fig. 6. Difference in cytokine profile between (A) peritoneal macrophages and (B) Kupffer cells in response to LPS *in vitro*. Kinetics of TNF-α, IL-12p40, and IL-10 production by peritoneal macrophages ($2 \times 10^6$/mL) and Kupffer cells ($1 \times 10^6$/mL) after stimulation with LPS (0.1 μg/mL) are shown. Culture supematants were collected at the indicated time points. TNF-α, IL-12p40, and IL-10 concentrations were determined via ELISA. Each value represents the mean ± SD of 4 experiments. $^*P < .01$ versus the sham-operated group. (■) BDL mice. (□) Sham-operated mice. TNF-α, tumor necrosis factor α; IL, interleukin.

lymphocytes, leading to subsidance of inflammatory reaction.[14,30] We have reported previously that IFN-γ is important for bacterial clearance after *E. coli* infection in mice.[31] In fact, we have shown in the present study that liver lymphocytes of sham-operated mice expressed abundant levels of IFN-γ mRNA after *E. coli* infection, although the serum level of IFN-γ was not detected even in sham-operated mice. On the other hand, those from BDL mice expressed only a marginal level of IFN-γ mRNA. Furthermore, *in vitro* IFN-γ production was significantly higher in liver lymphocytes of sham-operated mice when compared with those of BDL mice. These data strongly suggest that the predominant IL-10 production and concomitant suppression of IL-12 production by Kupffer cells in BDL mice might be responsible for host defense dysfunction against bacterial infection.

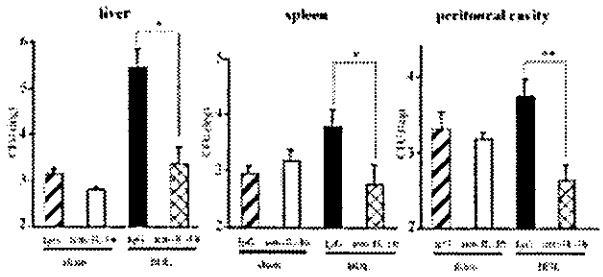


Fig. 7. The effect of neutralization of IL-10 in the course of *E. coli* infection. Sham-operated and BDL mice were injected intraperitoneally with anti-IL-10 neutralizing mAb (200 μg/mouse) 2 hours before *E. coli* challenge, and the numbers of the bacteria in liver, spleen, and peritoneal cavity were examined 24 hours after infection. $^*P < .05$; $^{**}P < .01$. CFU, colony-forming units; IgG, immunoglobulin G; IL, interleukin; BDL, bile duct ligation.

We have demonstrated that there is no significant difference in serum TNF-α production between sham and BDL mice after *E. coli* infection. In contrast, previous papers reported that BDL mice produced a large amount of TNF-α after LPS stimulation.[11,32] This may reflect a difference of LPS versus whole bacterial challenge. In fact, we found in our experimental model that serum TNF-α levels of BDL mice were more than 10 times higher than those of sham-operated mice 1 hour after 4 mg/kg LPS injection (data not shown).

A notable finding in this study is a difference in *ex vivo* production of IL-10 and IL-12 in response to LPS between Kupffer cells and peritoneal macrophages from BDL mice. We found that peritoneal macrophages from BDL mice were able to produce a large amount of IL-12 and TNF-α, whereas IL-10 production was prominent in Kupffer cells from BDL mice. These results suggest that cytokine production by Kupffer cells and peritoneal macrophages are differentially regulated by their milieu. Although serum factors in cholestasis (*e.g.*, increased concentrations of bile acids and bilirubin) are shown to affect functions of immune cells, it seems unlikely that

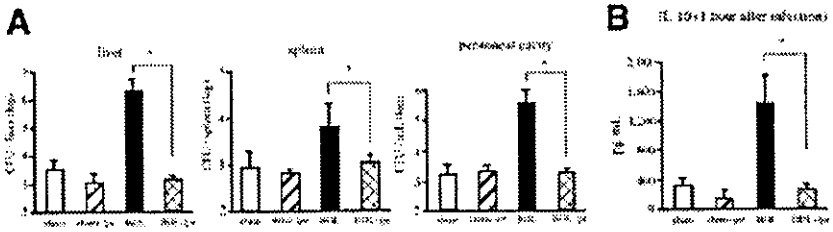


Fig. 8. Bacterial clearance in Fas-mutated *lpr* mice with BDL. (A) Bacterial clearances in organs 24 hours after *E. coli* challenge were counted in C57BL/6 and *lpr* mice. BDL-*lpr* mice did not show impaired bacterial clearance at the indicated time. Data are expressed as the mean ± SD for 5 mice. (B) Serum IL-10 production in *lpr* mice 1 hour after *E. coli* infection. Serum IL-10 level was lower in BDL-*lpr* mice compared with that in BDL mice. Results were derived from 5 mice per group. $*P < .05$. CFU, colony-forming units; BDL, bile duct ligation.

such serum factors are involved in the differential regulation of Kupffer cells and peritoneal macrophages.[1,33–35]

Kuppfer cells are shown to be activated by engulfing apoptotic hepatocytes induced by various stimuli.[20–23] Because macrophages are demonstrated to become capable of producing IL-10 after engulfing apoptotic bodies,[16,17] it is possible to speculate that Kupffer cells in cholestatic mice are also activated to generate IL-10 predominantly after ingesting increased apoptotic hepatocytes induced by BDL. To evaluate this possibility, we conducted a series of experiments using Fas-mutated *lpr* mice, which are demonstrated to be resistant to Fas-mediated hepatocyte apoptosis. We have shown that *lpr* mice are resistant to BDL-induced hepatocyte apoptosis and that *lpr* mice with BDL are able to kill *E. coli* efficiently to a similar extent to that of sham-operated mice, with a small amount of IL-10 production. These results strongly support the scenario that BDL induces predominant IL-10 production by Kupffer cells through ingesting Fas-mediated apoptosis of hepatocytes. It has also been demonstrated that Fas signaling in macrophages induces IL-10 gene expression.[36] We have recently reported that natural killer T cells in the liver express Fas-ligand directly through toll-like receptors induced by gram-negative bacteria such as *Salmonella choleraesuis* and *E. coli*.[37,38] Taken together, it also seems likely that Fas-expressing Kupffer cells in BDL mice are susceptible to signals via Fas-ligand expressed on natural killer T cells after *E. coli* infection and predominantly produce IL-10. Further studies are needed to clarify the mechanism of predominant IL-10 production by Kupffer cells in BDL mice.

In conclusion, increased IL-10 and reciprocally suppressed IL-12 production by Kupffer cells is responsible for deteriorated resistance to bacterial infection in BDL mice. Fas-mediated hepatocyte apoptosis may be involved in the predominant IL-10 production by Kupffer cells. These data support the clinical practice of biliary drainage before surgery to decrease perioperative septic complications. Moreover, our findings may provide a therapeutic approach to the control of cholestasis-associated bacterial infection.

*Acknowledgment:* The authors thank K. Itano, A. Nishikawa, and M. Yoshimura for their excellent technical assistance.

## References

1. Arai T, Yoshikai Y, Kamiya J, Nagino M, Uesaka K, Yuasa N, et al. Bilirubin impairs bactericidal activity of neutrophils through an antioxidant mechanism in vitro. J Surg Res 2001;96:107–113.
2. Scott-Conner CE, Grogan JB. The pathophysiology of biliary obstruction and its effect on phagocytic and immune function. J Surg Res 1994;57:316–336.
3. Jiang WG, Puntis MC. Immune dysfunction in patients with obstructive jaundice, mediators and implications for treatments. HPB Surg 1997;10:129–142.
4. Dixon JM, Armstrong CP, Duffy SW, Davies GC. Factors affecting morbidity and mortality after surgery for obstructive jaundice: a review of 373 patients. Gut 1983;24:845–852.
5. Kimmings AN, van Deventer SJ, Obertop H, Rauws EA, Gouma DJ. Inflammatory and immunologic effects of obstructive jaundice: pathogenesis and treatment. J Am Coll Surg 1995;181:567–581.
6. Deitch EA, Sittig K, Li M, Berg R, Specian RD. Obstructive jaundice promotes bacterial translocation from the gut. Am J Surg 1990;159:79–84.
7. Slocum MM, Sittig KM, Specian RD, Deitch EA. Absence of intestinal bile promotes bacterial translocation. Am Surg 1992;58:305–310.
8. Sheen-Chen SM, Chau P, Harris HW. Obstructive jaundice alters Kupffer cell function independent of bacterial translocation. J Surg Res 1998;80:205–209.
9. Bemelmans MH, Gouma DJ, Greve JW, Buurman WA. Cytokines tumor necrosis factor and interleukin-6 in experimental biliary obstruction in mice. HEPATOLOGY 1992;15:1132–1136.
10. Fujiwara Y, Shimada M, Yamashita Y, Adachi E, Shirabe K, Takenaka K, et al. Cytokine characteristics of jaundice in mouse liver. Cytokine 2001;13:188–191.
11. Harry D, Anand R, Holt S, Davies S, Marley R, Fernando B, et al. Increased sensitivity to endotoxemia in the bile duct-ligated cirrhotic rat. HEPATOLOGY 1999;30:1198–1205.
12. Lechner AJ, Velasquez A, Knudsen KR, Johanns CA, Tracy TF Jr, Matuschak GM. Cholestatic liver injury increases circulating TNF-alpha and IL-6 and mortality after Escherichia coli endotoxemia. Am J Respir Crit Care Med 1998;157:1550–1558.
13. Sewnath ME, Van Der Poll T, Ten Kate FJ, Van Noorden CJ, Gouma DJ. Interleukin-1 receptor type 1 gene-deficient bile duct-ligated mice are partially protected against endotoxin. HEPATOLOGY 2002;35:149–158.
14. Moore KW, de Waal Malefyt R, Coffman RL, O'Garra A. Interleukin-10 and the interleukin-10 receptor. Annu Rev Immunol 2001;19:683–765.

15. Takano M, Nishimura H, Kimura Y, Washizu J, Mokuno Y, Nimura Y, et al. Prostaglandin E2 protects against liver injury after Escherichia coli infection but hampers the resolution of the infection in mice. J Immunol 1998;161:3019–3025.
16. Savill J, Fadok V. Corpse clearance defines the meaning of cell death. Nature 2000;407:784–788.
17. Byrne A, Reen DJ. Lipopolysaccharide induces rapid production of IL-10 by monocytes in the presence of apoptotic neutrophils. J Immunol 2002; 168:1968–1977.
18. Arai T, Hiromatsu K, Kobayashi N, Takano M, Ishida H, Nimura Y, et al. IL-10 is involved in the protective effect of dibutyryl cyclic adenosine monophosphate on endotoxin-induced inflammatory liver injury. J Immunol 1995;155:5743–5749.
19. Miyoshi H, Rust C, Roberts PJ, Burgart LJ, Gores GJ. Hepatocyte apoptosis after bile duct ligation in the mouse involves Fas. Gastroenterology 1999;117:669–677.
20. Faa G, Ledda-Columbano GM, Ambu R, Congiu T, Coni P, Riva A, et al. An electron microscopic study of apoptosis induced by cycloheximide in rat liver. Liver 1994;14:270–278.
21. Canbay A, Feldstein AE, Higuchi H, Werneburg N, Grambihler A, Bronk SF, et al. Kupffer cell engulfment of apoptotic bodies stimulates death ligand and cytokine expression. HEPATOLOGY 2003;38:1188–1198.
22. Dini L, Pagliara P, Carla EC. Phagocytosis of apoptotic cells by liver: a morphological study. Microsc Res Tech 2002;57:530–540.
23. Ruzittu M, Carla EC, Montinari MR, Maietta G, Dini L. Modulation of cell surface expression of liver carbohydrate receptors during in vivo induction of apoptosis with lead nitrate. Cell Tissue Res 1999;298:105–112.
24. Braet F, De Zanger R, Sasaoki T, Baekeland M, Janssens P, Smedsrod B, et al. Assessment of a method of isolation, purification, and cultivation of rat liver sinusoidal endothelial cells. Lab Invest 1994;70:944–952.
25. Su GL, Klein RD, Aminlari A, Zhang HY, Steinstraesser L, Alarcon WH, et al. Kupffer cell activation by lipopolysaccharide in rats: role for lipopolysaccharide binding protein and toll-like receptor 4. HEPATOLOGY 2000;31: 932–936.
26. Matsuguchi T, Musikacharoen T, Ogawa T, Yoshikai Y. Gene expressions of Toll-like receptor 2, but not Toll-like receptor 4, is induced by LPS and inflammatory cytokines in mouse macrophages. J Immunol 2000;165: 5767–5772.
27. Scott-Conner CE, Grogan JB, Scher KS, Bernstein J. Impaired clearance of Escherichia coli bacteremia in early biliary obstruction. Am J Surg 1989; 157:210–214.
28. Tomioka M, Iinuma H, Okinaga K. Impaired Kupffer cell function and effect of immunotherapy in obstructive jaundice. J Surg Res 2000;92:276–282.
29. Canbay A, Higuchi H, Bronk SF, Taniai M, Sebo TJ, Gores GJ. Fas enhances fibrogenesis in the bile duct ligated mouse: a link between apoptosis and fibrosis. Gastroenterology 2002;123:1323–1330.
30. Yoshimoto T, Takeda K, Tanaka T, Ohkusu K, Kashiwamura S, Okamura H, et al. IL-12 up-regulates IL-18 receptor expression on T cells, Th1 cells, and B cells: synergism with IL-18 for IFN-gamma production. J Immunol 1998;161:3400–3407.
31. Takano M, Nishimura H, Kimura Y, Mokuno Y, Washizu J, Itohara S, et al. Protective roles of gamma delta T cells and interleukin-15 in Escherichia coli infection in mice. Infect Immun 1998;66:3270–3278.
32. McCullough LK, Takahashi Y, Le T, Pittman QJ, Swain MG. Attenuated febrile response to lipopolysaccharide in rats with biliary obstruction. Am J Physiol Gastrointest Liver Physiol 2000;279:G172–G177.
33. Calmus Y, Guechot J, Podevin P, Bonnefis MT, Giboudeau J, Poupon R. Differential effects of chenodeoxycholic and ursodeoxycholic acids on interleukin 1, interleukin 6 and tumor necrosis factor-alpha production by monocytes. HEPATOLOGY 1992;16:719–723.
34. Gianni L, Di Padova F, Zuin M, Podda M. Bile acid-induced inhibition of the lymphoproliferative response to phytohemagglutinin and pokeweed mitogen: an in vitro study. Gastroenterology 1980;78:231–235.
35. Hillaire S, Boucher E, Calmus Y, Gane P, Ballet F, Franco D, et al. Effects of bile acids and cholestasis on major histocompatibility complex class I in human and rat hepatocytes. Gastroenterology 1994;107:781–788.
36. Daigle I, Ruckert B, Schnetzler G, Simon HU. Induction of the IL-10 gene via the fas receptor in monocytes—an anti-inflammatory mechanism in the absence of apoptosis. Eur J Immunol 2000;30:2991–2997.
37. Shimizu H, Matsuguchi T, Fukuda Y, Nakano I, Hayakawa T, Takeuchi O, et al. Toll-like receptor 2 contributes to liver injury by Salmonella infection through Fas ligand expression on NKT cells in mice. Gastroenterology 2002;123:1265–1277.
38. Hiromatsu T, Matsuguchi T, Shimizu H, Yajima T, Nishimura H, Arai T, et al. NK T cells stimulated with a ligand for TLR2 at least partly contribute to liver injury caused by Escherichia coli infection in mice. Eur J Immunol 2003;33:2511–2519.

# The Interaction between GATA Proteins and Activator Protein-1 Promotes the Transcription of *IL-13* in Mast Cells[1]

**Akio Masuda,[2]* Yasunobu Yoshikai,[‡] Hiroaki Kume,[†] and Tetsuya Matsuguchi[§]**

**IL-13 is considered to be a key modulator in the pathogenesis of Th2-induced allergic inflammation, although little is known about the regulation of *IL-13* transcription in mast cells. In T cells, involvement of GATA-3 in cell type-specific expression of the *IL-13* gene has been reported. However, the mechanisms that induce rapid transactivation of the *IL-13* gene in response to various types of stimulation have hitherto remained unknown. In this report, we describe our investigation of the promoter region necessary for *IL-13* transcription; we have found that both AP-1 and GATA proteins are indispensable for *IL-13* transcription in mouse mast cells. In our investigation, we focused on the functional interaction between GATA and AP-1 in the *IL-13* promoter context. Transfection experiments have revealed that GATA-1 and GATA-2 proteins are able to associate with AP-1 proteins. We have also shown that overexpression of GATA-1 induced excess AP-1 binding to the *IL-13* promoter as well as a significant increase in IL-13 production in mast cells. The results of the present study have shown that direct interaction between AP-1 and GATA proteins plays an important role in *IL-13* transcription in mast cells.** *The Journal of Immunology,* **2004, 173: 5564–5573.**

Interleukin 13 is a pleiotropic 12-kDa product of a gene on chromosome 5 at q31, which was originally described as being produced by activated Th 2 cells, but its expression by activated mast cells has also been reported (1–4). By using the IL-4Rα chain and STAT6 for signaling, IL-13 shares some biological activities with IL-4, such as the promotion of human B cell growth and the switching of B cells to the IgE isotype (5). Furthermore, it has been shown that IL-13 is a critical mediator in experimental models of allergic asthma (6, 7). Thus, IL-13 is considered to be the key modulator in the pathogenesis of Th2-induced allergic inflammation (8).

Although the mechanisms that regulate IL-13 production in T cells or mast cells remain largely unknown, it has been reported that GATA-3 plays an important role in IL-13 production in T cells (9). GATA-3 has been reported to be involved in the chromatin remodeling of Th2 cytokine genes and the improvement in the accessibility of transcriptional factors to promoter regions of Th2 cytokines (10). Furthermore, it has recently been reported that GATA-3 binding sites in the proximal *IL-13* promoter are necessary for cell type-specific expression of IL-13 (11). However, the mechanisms that activate *IL-13* transcription immediately in response to stimulation are still underexplored. Although rapid phosphorylation of GATA proteins after various types of stimulation has been reported, the role of these phosphorylations in transcriptional regulation is still controversial (12, 13). Furthermore, almost nothing is known about the regulation of *IL-13* gene in mast cells. Mast cells have high expression levels of GATA-1 and GATA-2 but little expression of GATA-3, and the roles of GATA-1 and GATA-2 in *IL-13* transcription have not been explored (14, 15).

GATA proteins are tissue-restricted transcription factors that bind a WGATAR DNA motif through a zinc-finger DNA-binding domain. Based on sequence homology and expression patterns, GATA proteins have been divided into two subfamilies, GATA-1–3 and GATA-4–6 (16). The former family is prominently expressed in hemopoietic stem cells, and the latter family is expressed in various mesoderm- and endoderm-derived tissues (17). GATA-1 and GATA-2 are expressed in mast cells, erythroblasts, and megakaryocytes (14, 18), and are instrumental for tissue-specific gene expression. Genes that are selectively expressed in mast cells and whose expression depends on GATA proteins include those encoding carboxypeptidase A, several mast cell-specific proteases and the IgE receptor α- and β-chains (14, 19–21). Furthermore, GATA-1 and -2 play important roles in the transcription of Th2 cytokine genes such as IL-4 and IL-5 in mast cells (22, 23).

Several observations suggest that AP-1, which is a dimeric complex of a Jun family protein and a Fos family protein, may functionally interact with GATA proteins. First, GATA and AP-1 sites are found in close association in the core hypersensitivity sites of the globin locus control region and in a number of erythroid promoters (24, 25). Second, a number of experiments have indicated that GATA sites in conjunction with an AP-1 site constitute an active promoter, whereas GATA sites in conjunction with a TATA box alone do not form an active promoter (25, 26). In the promoter of the endothelin-1 gene, the Jun/Fos heterodimer was found to cooperate with GATA-2 in the activation of transcription (27). Moreover, the IL-5 promoter has been shown to require both AP-1 and GATA elements for its activity in T cells (28).

In our present study, we have investigated the promoter region necessary for IL-13 transcription and found that AP-1 and GATA binding sites are indispensable for IL-13 transcription. We focused on the functional interaction between GATA and AP-1 in the *IL-13* promoter context. Transfection experiments revealed that GATA-1 and GATA-2 proteins are able to associate with AP-1 proteins. We also found that overexpression of GATA-1 induced excess binding

*Division of Host Defense, Center for Neural Disease and Cancer, and †Division of Respiratory Diseases, Department of Internal Medicine, Nagoya University Graduate School of Medicine, Nagoya, Japan; ‡Division of Host Defense, Research Center for Prevention of Infectious Diseases, Medical Institute of Bioregulation, Kyushu University, Fukuoka, Japan; and §Division of Biochemistry and Molecular Dentistry, Department of Developmental Medicine, Graduate School of Medical and Dental Sciences, Kagoshima University, Kagoshima, Japan

Received for publication March 25, 2004. Accepted for publication August 20, 2004.

The costs of publication of this article were defrayed in part by the payment of page charges. This article must therefore be hereby marked *advertisement* in accordance with 18 U.S.C. Section 1734 solely to indicate this fact.

[1] This work was supported in part by grants from the Japanese Society for the Promotion of Science and Japanese Allergy Foundation.

[2] Address correspondence and reprint requests to Dr. Akio Masuda, Division of Host Defense, Center for Neural Disease and Cancer, Nagoya University Graduate School of Medicine, 65, Tsurumai-cho, Showa-ku, Nagoya 466-8550, Japan. E-mail address: amasuda@med.nagoya-u.ac.jp



0022-1767/04/$02.00

of AP-1 to the *IL-13* promoter as well as a significant increase in IL-13 production.

## Materials and Methods

### *Reagents and Abs*

RPMI 1640 medium and FCS were purchased from Sigma-Aldrich (St. Louis, MO). LPS from *Escherichia coli* serotype 055:B5, the mouse monoclonal anti-DNP Ab, the DNP-human serum albumin, ionomycin, and PMA were obtained from Sigma-Aldrich. Anti-histone H3 Ab, anti-Myc mAb, anti-Flag M2 mAb, anti-Jun polyclonal Ab, anti-*fos* polyclonal Ab, anti-GATA-1 mAb, and anti-GATA-2 mAb were purchased from Santa Cruz Biotechnology (Santa Cruz, CA).

### *Cells*

The MC/9 mouse mast cell line was cultured as previously described (29). The PT18 mouse mast cell line was kindly provided from Dr. K. Okumura (Juntendo University, Tokyo, Japan). The P815 mouse mastcytoma cells were obtained from Cell Resource Center for Biomedical Research (Tohoku University, Sendai, Japan). These cells were grown in RPMI 1640 with 10% FCS. Bone marrow-derived mast cells (BMMCs)[3] were derived from femoral bone marrow cells of 6-wk-old BALB/c mice. After 3 wk of culture with 10% WEHI-3-conditioned medium, the cells were harvested for the experiments and consisted of >98% mast cells assessed by toluidine blue staining.

A human embryonic kidney cell line, HEK 293T, was maintained in DMEM with 10% FCS. Cells were washed twice and incubated in fresh culture medium for 6 h and stimulated with PMA (10 ng/ml) plus ionomycin (1 μg/ml) or LPS (1 μg/ml) unless otherwise indicated. For the cross-linking of FcεRI on mast cells, cells were sensitized by incubation for 2 h with 1 μg/ml anti-DNP IgE in RPMI 1640 containing 10% FCS, washed, incubated ($2 \times 10^6$ cells/ml) for 6 h in RPMI 1640 containing 10% FCS, and stimulated with 10 ng/ml DNP-human serum albumin.

### *IL-13 promoter constructs*

DNA fragments of the murine IL-13 promoter were amplified by PCR using the primers: senses CGGGGTACCGGGGTAGGGGAGCTGAATAG (pGL3–2024), CGGGGTACCGCTGTCATGTTTTCCCCAGT (pGL3–1253), CGGGGTACCGAGTTCAAGCTGCCCACTG (pGL3–705), CGGGGTACCATAGTGTGGTTGGAAGTGGC (pGL3–560), CGGGGT ACCGAAAGGAAGGAAGGGAGGAA (pGL3–428), CGGGGTACCGTG TCAAGGGGTCAGCATT (pGL3–322), CGGGGTACCTCTTTCCTT TAGCGGCCAC (pGL3–156), CGGGGTACCAAGATGAGTAAAG ATGTGG (pGL3–106), CGGGGTACCGATGTGGTTTTCAGATA (pGL3–94), CGGGGTACCGTGAGGCGTCATCACTTTGG (pGL3–51), and an antisense TCCGCTCGAGTGAGAGAACCAGGGAGCTGT. All PCR products were then cloned into a pGEMTeasy vector (Promega, Madison, WI) and digested with *Xho*I and *Kpn*I, and the inserts were subcloned into a pGL3-basic vector (Promega). The mutations of the promoter region between −106 and −94 were prepared by ligating two PCR products amplified by primers: sense CGGGGTACCGAGTTCAAGCTGCCCACTG, antisense GCTAGCA TTTTTTTTTTTCTTTTTTGG (Mut1) or GCTAGCATCTTGAATTTTT TTTTTTCTTTTTTGG (Mut2), and sense GCTAGCTGAGTAAAGATGT GGTTTTC (Mut1) or GCTAGCAGATGTGGTTTTCAGATAATGCCC (Mut2) and antisense TCCGCTCGAGTGAGAGAACCAGGGAGCTGT; after *Nhe*I digestion. The ligated DNA fragment was cloned into a pGL3 luciferase vector.

***Mammalian expression plasmids.*** The expression plasmids for the Myc-tagged mouse GATA-1 and GATA-2 were prepared by cloning the mouse GATA-1 or GATA-2 cDNAs inserted into pBluescript KS (+) vectors. A series of mouse GATA-1 deletion mutants was prepared by PCR from pEFBOS-Myc GATA-1 as the template using the sense primers: ACGCG TATGGAGGGAATTCCTGGGG (Δ1–86), ACGCGTCCATTGGCCCC TTGTGAG (ΔN and ΔN + C), ACGCGTCCCATGGATTTTCCTGGTC (ΔC), GGCGCGCCTTGTCAGCAAACGGGCAGGC (ΔN + C + NF) and antisense primers: ACGCGTTCAAGAACTGAGTGGGGC (Δ1–86 and ΔN), GGCGCGCCCCCCGCTTCTTTTTCCCTTT (ΔC, ΔN + C, and ΔN + C + NF); after *Mlu*I or *Asc*I digestion, PCR products were cloned into the pEFBOS-Flag or pEFBOS-Myc vector. ΔNF and ΔCF plasmids were prepared by ligating two PCR products amplified by primers: sense ACGCGTCCCATGGATTTTCCTGGTC, antisense CTCGAGACAAGG GGCCAATGGCAGGC (ΔNF) CTCGAGGCTGCCCGTTTGCTGACAAT (ΔCF), and sense CTCGAGATTGTCAGCAAACGGGCAGG (ΔN) CTC GAGAAGCTCCATCAGGTGAACCG (ΔC), antisense ACGCGTTCAAG AACTGAGTGGGGC; after *Xho*I digestion. The ligated DNA fragment was cloned into pEFBOS-Myc vector. The expression plasmid for mouse c-*jun* (pEFBOS-Flag-c-*jun*) and N-terminal deletion mutants (pEFBOS-Myc-DN-c-*jun*) were prepared by RT-PCR using the sense primer: ACGCGTATGAC TGCAAAGATGGAAAC (c-*jun*), ACGCGTAGCCAGAACACGCTTCCC AGT (DN-c-*jun*), and antisense primer: ACGCGTTCAAAACGTTTGCA ACTGCT. PCR products, digested with *Mlu*I, were subcloned into the pEFBOS-Flag or pEFBOS-Myc vector. All plasmid constructs were verified by restriction enzyme mapping and nucleotide sequencing. pAP-1 Luc, which is designed for monitoring induction of AP-1, were purchased from BD Clontech (Palo Alto, CA).

### *Transfection and luciferase assay*

Cells were transiently transfected with 3.5 μg of *IL-13* promoter/luciferase plasmid and 0.1 μg of pRL/SV40 (an internal control) by DMRIE-C Reagent (Invitrogen Life Technologies, Carlsbad, CA) according to the manufacturer's instructions. When indicated, cells were cotransfected with the indicated amount of GATA or c-*jun* expression vector or an empty vector with 1 μg of the *IL-13* promoter/luciferase plasmid. Forty-eight hours after the transfection, the cells were stimulated for 12 h. The luciferase activity was measured by using the Dual-Luciferase Reporter Assay System (Toyo Ink, Tokyo, Japan) according to the manufacturer's instructions. HEK293T cells were transiently transfected with a combination of expression plasmids (2 μg total/plate) by LipofectAMINE (Invitrogen Life Technologies) according to the manufacturer's instructions.

### *Immunoblotting, immunoprecipitation, and DNA-binding protein purification*

Nuclear and cytoplasmic lysate preparation, immunoblotting, and immunoprecipitation were performed as previously described (30, 31). AP-1 and associating proteins were harvested using a DNA-binding protein purification kit (Roche, Basel, Switzerland) according to the manufacturer's instruction. The kit contains magnetic particles coupled to a double-stranded oligonucleotide. To this tethered oligonucleotide, double-stranded oligonucleotides containing the sequence for AP-1-binding were ligated. The sequences of oligonucleotides are as follows: sense CTAGTGATGAGTCAGCCGGAT (AP-1), GCTTACAATGAAGGCTTACAATGAAG (scramble), and antisense ATC CGGCTGACTCATCACTAG (AP-1), CTTCATTGTAAGCCTTCATTG TAAGC (scramble). Nuclear extracts were applied to the magnetic particles, and the oligo-particle complex captured the AP-1 protein. Separation of the bound protein from the supernatant was performed with a magnetic separator and washing steps. The purified proteins were eluted with a buffer of high ionic strength.

### *EMSA*

Nuclear extracts were prepared as previously described (30). The double-strand DNA fragment carrying the region between −108 and −94 of the mouse *IL-13* gene 5′ upstream region was prepared by annealing two oligonucleotides: sense TTCAAGATGAGTAAA and antisense TTTACT CATCTTGAA, followed by $^{32}P$ labeling by T4 nucleotide kinase. The sequences of mutated version were as follows: sense TGCTAGCTGAG TAAA (Mut1), TTCAAGATGGCTAGC (Mut2), and antisense TTTACT CAGCTAGCA (Mut1), GCTAGCCATCTTGAA (Mut2). Nuclear extracts (5 μg of total protein) were incubated with the $^{32}P$-labeled double-stranded probe. For competition assays, nuclear extracts were incubated with a 50-fold molar excess of the unlabeled probe before the addition of the $^{32}P$-labeled probe. For the supershift experiment, 1 μg of the indicated Ab was incubated with nuclear extracts for 2 h before the binding reaction. Samples were run on a 5% nondenaturing polyacrylamide gel in Tris/glycine/EDTA buffer. The gel was dried and visualized by autoradiography.

### *Chromatin immunoprecipitation (ChIP) assay*

A ChIP assay was performed as previously described (32). The chromatin, sheared by sonication was immunoprecipitated with anti-*fos* Ab overnight at 4°C. Harvested DNAs were PCR amplified in a final volume of 50 μl containing 2.5 mmol/L magnesium dichloride, 2.5 U (AmpliTaq; PerkinElmer, Wellesley, MA), and 1 μmol/L-specific primers. The *IL-13* promoter-specific primers are as follows (−156 to +52): sense, AAGAT GAGTAAAGATGTGG; antisense, TGAGAGAACCAGGGAGCTGT. The downstream of *IL-13* promoter-specific primers are as follows (+2943 to +3138): sense, ATGAGTCTGTCAGTGTCCCG; antisense, CCGTGGCA GACAGGAGTGTT. PCR conditions are as follows: 94°C for 5 min; 94°C for 45 s; 60°C for 45 s; 72°C for 45 s; and 72°C for 7 min. PCR was done for 27 cycles. Five microliters of each PCR product were run on a 2% agarose gel for

[3] Abbreviations used in this paper: BMMC, bone marrow-derived mast cell; ChIP, chromatin immunoprecipitation.

UV visualization. For each reaction, 1% of cross-link released chromatin was saved and used as input control.

*Cytokine ELISA*

The cell-free culture supernatants were measured for the concentration of IL-13 (BD Pharmingen, San Diego, CA) by ELISA according to the manufacturer's instructions.

*Generation of stable transfectants*

P815 cells were transfected with 3 μg of pEFBOS-Myc-GATA-1 vector along with 1 μg of pCDNA3 plasmid (Invitrogen Life Technologies). Transfectants were selected with G418 (0.8 μg/ml). After 4 wk, resistant clones were screened for the right-sized protein expression by Western blotting.

*Statistical analysis*

The statistical significance of the data was determined by the Student's *t* test. A $p$ value of $<0.05$ was taken as significant.

## Results

*Structural and functional analysis of the 5′-upstream region of the murine* IL-13 *gene in mast cell lines*

To investigate the mechanism of IL-13 transcription in mast cells, we examined three well-established mast cell lines, MC/9 cells, PT18 cells, and P815 cells. These cell lines were stimulated with LPS, IgE cross-linking, or PMA/ionomycin, and we confirmed that MC/9 cells, as well as BMMCs, produced IL-13 in response to all of these three stimulations, and that PT18 and P815 cells responded only to stimulation by PMA/ionomycin (Fig. 1*A*).

A series of 5′-deletion constructs of the murine *IL-13* promoter region was initially generated to analyze *IL-13* promoter activity and to identify functional *cis*-acting elements required for *IL-13* gene expression. These 5′-deleted DNAs were cloned into the promoterless luciferase reporter vector pGL3-basic. The PT18 cells, transfected with the generated plasmids, were stimulated with PMA/ionomycin for 12 h, and luciferase activities were measured.

As shown in Fig. 1*B*, the highest induction was obtained with pGL3–2024 for PMA/ionomycin treatment. Four shorter constructs (1253, 705, 560, and 428) showed similar induction levels for PMA/ionomycin treatment. However, further deletion down to 322 caused a reduction in activity, and responsiveness was abrogated when the construct was deleted down to −51. Next, we made two constructs (−106 and −94) and examined the promoter activities of constructs shorter than −428 after PMA/ionomycin stimulation in PT18 cells. As shown in Fig. 1*C*, responsiveness was abrogated when the construct was deleted down to −94 (pGL3–94).

These constructs were also transfected into MC/9 cells and P815 cells. As shown in Fig. 1*D*, the results of MC/9 cells stimulated with PMA/ionomycin were similar to those of PT18 cells. The degree of response to this treatment was reduced with the reduction in the length of the construct, and was abrogated when the construct was shortened down to −94. In the case of stimulation by IgE cross-linking and LPS, the responsiveness of luciferase activity was maintained until the construct was shortened to −106 but was abrogated at −94. The high degree of inducibility through PMA/ionomycin stimulations and low degree of inducibility through IgE cross-linking and LPS stimulations were considered to reflect the production levels of IL-13, as shown in Fig. 1*A*. The luciferase activities of P815 cells were similar to those of PT18 cells and MC/9 cells. As shown in Fig. 1*E*, responsiveness was abrogated when the construct was deleted down to −94 (pGL3–94). These findings suggest that the fragment from −106 to the +62 fragment contains the minimal murine *IL-13* promoter, and that the promoter region between −106 and −94 plays an important role in the induction of *IL-13* promoter activity in mast cells.

*The role of the promoter region between −106 and −94 in murine* IL-13 *gene expression in mast cells*

A search in the nucleotide sequence upstream of the transcriptional start sites for the potential binding sites of transcriptional factors was conducted using TRANSFAC (http://www.motif.genome.ad.jp; cutoff score = 80), and GATA and AP-1 binding sites were found in the region between −106 and −94. To confirm that the promoter region between −106 and −94 is functionally involved in *IL-13* transcription, we made two constructs based on the pGL-705 construct, which we designated Mut1 and Mut2, and compared their activities with the activity of pGL-705. The TRANSFAC program predicted that Mut1 would show a reduced GATA binding potential as the score is reduced from 84 to 68, but would show an increased AP-1-binding potential as the score is slightly raised from 82 to 85. In the case of Mut2, the program predicted reduced AP-1-binding potential (the score was reduced from 82 to 55) and increased GATA-binding potential (the score was raised from 84 to 90). As shown in Fig. 2*B*, each mutant construct showed a significant reduction of promoter activity in response to PMA/ionomycin in both PT18 and MC/9 cells. A reduction of promoter activity was also confirmed in P815 cells (Fig. 2*B*). These findings indicate the functional involvement of GATA or AP-1 in the *IL-13* promoter region between −106 and −94.

*Identification of GATA-1, GATA-2, and the AP-1 complex binding to the* IL-13 *promoter in mast cells by EMSA*

EMSA was conducted to determine whether protein-DNA binding within the region between −106 and −94 is involved in the activation of the *IL-13* promoter. Nuclear extracts prepared from PT18 cells stimulated with PMA/ionomycin or not were incubated with a $^{32}$P-labeled probe spanning the *IL-13* promoter region between −108 and −94. EMSA revealed the presence of two protein complexes binding to the probe (Fig. 3*A*). While the faster complex appeared constitutively, the slower one appeared after PMA/ionomycin stimulation. These two complexes were also observed in BMMCs and MC/9 cells, which were stimulated with LPS, IgE cross-linking, or PMA/ionomycin (Fig. 3*A*).

As shown in Fig. 3*B*, the introduction of mutations into the sequence of this probe (Mut1 and Mut2, which are described in Fig. 2*A*), reduced both faster and slower migrations of complexes, although Mut1 reduced faster migrations and Mut2 reduced slower migrations more efficiently.

To further confirm the components of these two protein-DNA complexes, Abs against GATA and AP-1 were added in the EMSAs. It has been reported that mast cells show high expression of GATA-1 and GATA-2, but not GATA-3 (14, 15). We also confirmed by Northern blotting that PT18 cells and MC/9 cells express GATA-1 and GATA-2 but not GATA-3 (data not shown). As shown in Fig. 3*C*, a combination of Abs against AP-1 subunits (at Fos and at Jun) efficiently abrogated or supershifted the inducible slower complexes. In contrast, a combination of Abs against GATA-1 and GATA-2 efficiently abrogated both the faster migrations and the slower migrations. These findings demonstrate that Jun/Fos complexes constitute the slower migrations and GATA-1 and GATA-2 account for both the slower and the faster migrations. Taken together, these findings indicate that GATA-1 and GATA-2 bind to the region between −106 and −94 constitutively, and AP-1 binds only after stimulation.

*AP-1 activities are indispensable for the activation of the* IL-13 *promoter*

To investigate the role of AP-1 in *IL-13* transcription in mast cells, we transfected an expression plasmid encoding an N-terminally

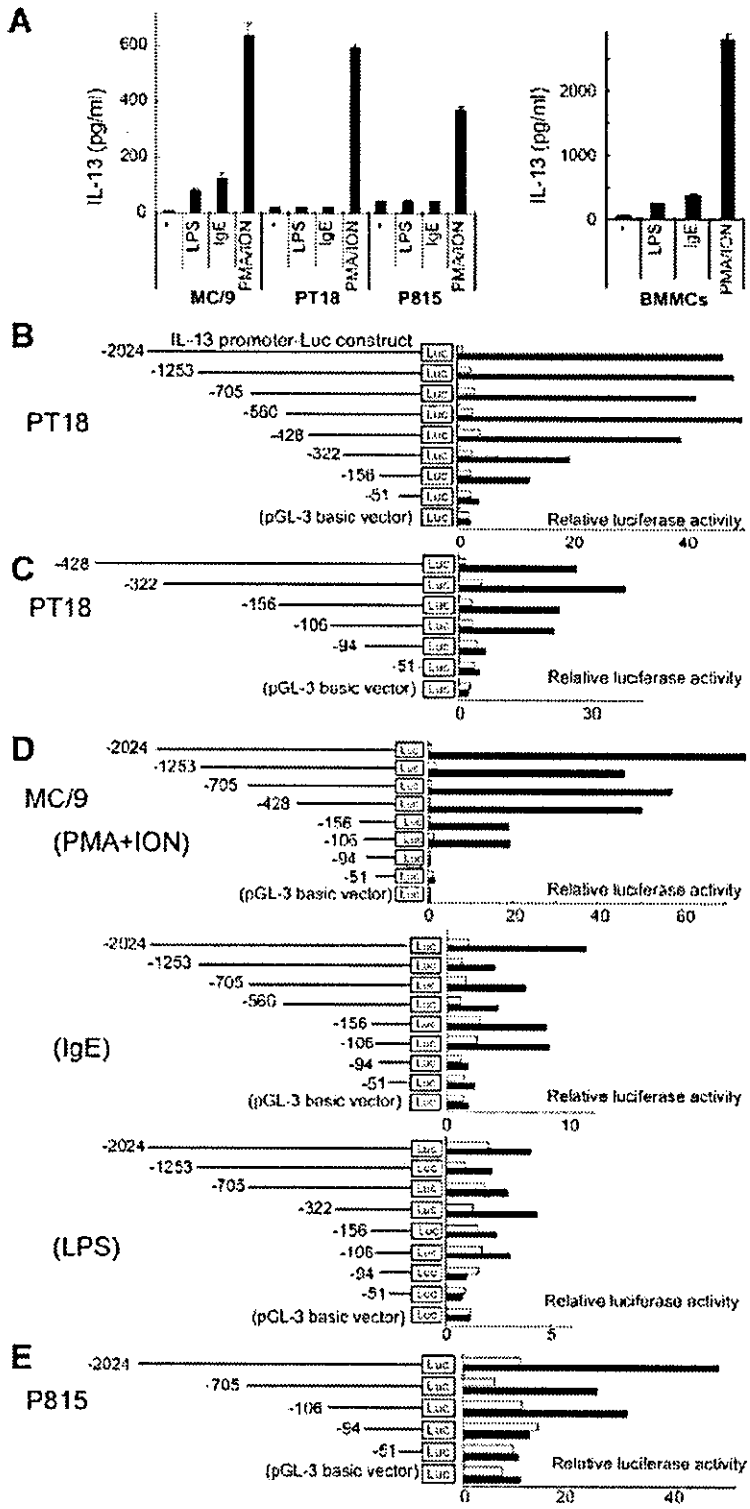


**FIGURE 1.** The structural and functional analysis of the 5′-upstream region of the murine *IL-13* gene. *A*, IL-13 production from mast cell lines. Cells ($2 \times 10^6$ cells/ml) were stimulated with LPS, IgE cross-linking, or PMA/ionomycin. After 16 h, the cell-free culture supernatants were collected and cytokine ELISAs were performed. The error bars represent SD values. *B–D*, PT18 cells, MC/9 cells, and P815 cells were transiently transfected with 3.5 μg of *IL-13* promoter/luciferase plasmid and 0.1 μg of pRL/SV40 (an internal control). *B* and *C*, PT18 cells were stimulated with PMA/ionomycin, (*D*) MC/9 cells were stimulated with PMA/ionomycin, IgE cross-linking, or LPS, and (*E*) P815 cells were stimulated with PMA/ionomycin. After 12 h, luciferase activities were measured. Units of luciferase activity were normalized based on values of pRL/SV40 activity for transfection activity (relative luciferase activity). □, Unstimulated, and, ■, stimulated conditions. A typical result of at least three independent experiments is shown. The result in *C* was confirmed in transfections using two independent preparations of each construct.

truncated form of c-*jun* (DN-c-*jun*), which has been reported to work in a dominant-negative fashion (33). We confirmed that DN-c-*jun* inhibits AP-1 activity in PT18 cells in a dose-dependent manner (Fig. 4*A*). We then transiently transfected pGL-106 with DN-c-*jun* or control vector into PT18 cells and stimulated the cells with PMA/ionomycin for 12 h. As shown in Fig. 4*B*, the induction of luciferase activity was significantly reduced by DN-c-*jun*. These findings suggest that AP-1 activity plays a critical role in the transcriptional activation of the *IL-13* gene.

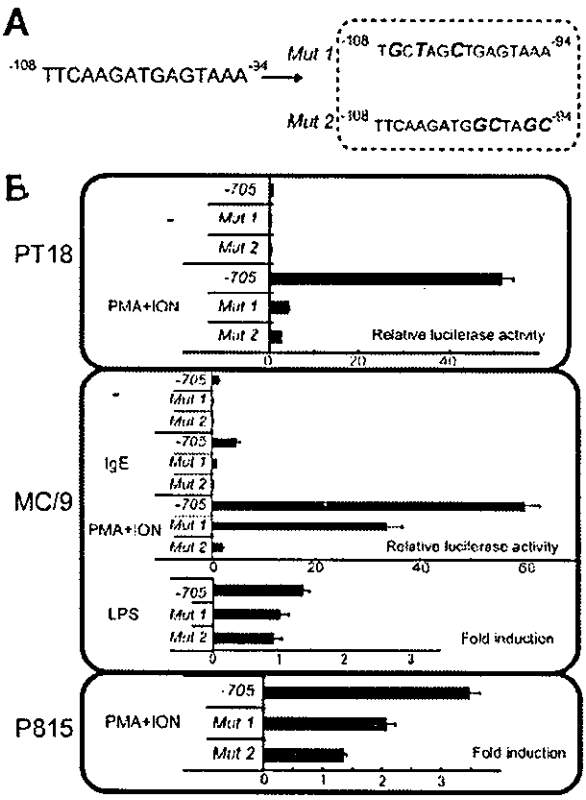


**FIGURE 2.** The role of the promoter region between −106 and −94 in *IL-13* gene expression in mast cells. *A*, Sequences of the promoter region between −108 and −94 in the *IL-13* gene. The altered sequences of this region in Mut1 or Mut2 are indicated in bold italic font. *B*, PT18, MC/9, and P815 cells were transiently transfected with 3.5 μg of *IL-13* promoter/luciferase plasmid and 0.1 μg of pRL/SV40. PT18 cells and P815 cells were stimulated with PMA/ionomycin. MC/9 cells were stimulated with PMA/ionomycin, IgE cross-linking, or LPS. After 12 h, luciferase activities were measured. Units of luciferase activity were normalized based on values of pRL/SV40 activity for transfection activity (relative luciferase activity). The fold inductions were calculated as follows: (relative luciferase activity of stimulated cells)/(relative luciferase activity of unstimulated cells). A typical result of at least three independent experiments is shown.

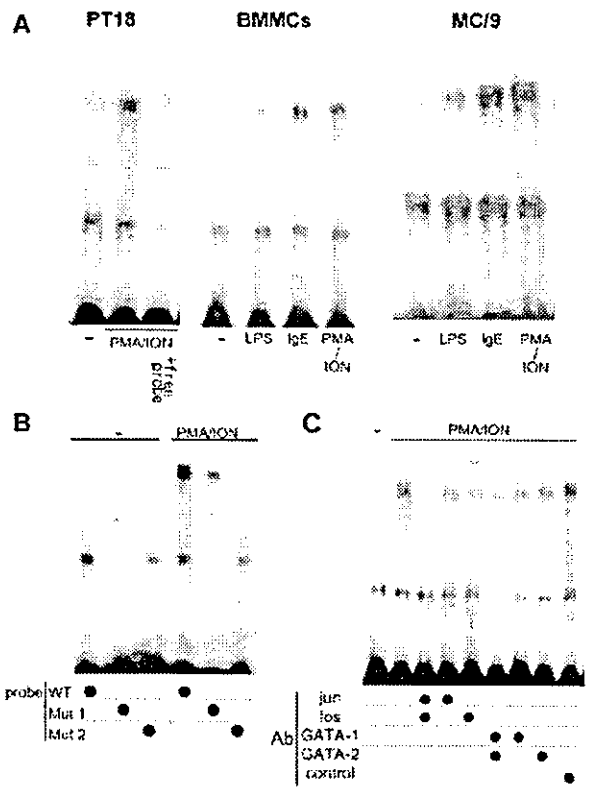


**FIGURE 3.** Identification of GATA-1, GATA-2, and AP-1 complex binding to the *IL-13* promoter in mast cells by EMSA. Cells were left untreated (−) or stimulated with PMA/ionomycin, IgE cross-linking, or LPS (1 μg/ml) for 20 min and nuclear extracts were prepared. *A*, EMSAs were performed by using $^{32}$P-labeled probe spanning the region between −108 and −94 of the *IL-13* promoter. For competition assays, nuclear extracts were incubated with a 50-fold molar excess of the unlabeled probe before the addition of $^{32}$P-labeled probe (+free probe). *B*, EMSA was performed with the nuclear extract of PT18 cells. $^{32}$P-labeled probe spanning the region between −108 and −94 of the *IL-13* promoter or $^{32}$P-probes that were introduced mutations (Mut1 or Mut2) were used as a probe. *C*, EMSA was performed with the nuclear extract of PT18 cells. The $^{32}$P-labeled probe spanning the region between −108 and −94 of the *IL-13* promoter was used as a probe. One microgram of the indicated Abs or isotype match Abs (control) were incubated with nuclear extracts for 2 h before the binding reaction.

### *Both GATA-1 and GATA-2 transactivate the* IL-13 *promoter through AP-1 activity*

As shown in Fig. 3, not only AP-1 but also GATA-1 and GATA-2 bind to the region between −106 and −94 in the *IL-13* promoter that is involved in transactivation of the *IL-13* gene. To examine the ability of GATA-1 and GATA-2 to transactivate the *IL-13* promoter, GATA-1 or GATA-2 expression plasmids were transfected in combination with pGL-106, and luciferase activity was measured after various stimulations. In MC/9 cells stimulated with IgE cross-linking or PMA/ionomycin, both GATA-1 and GATA-2 transactivated the *IL-13* promoter in a dose-dependent manner. Basal luciferase activity was also up-regulated by overexpression of either GATA-1 or GATA-2. Similar results were obtained with P815 cells (Fig. 4*C*).

To further confirm the role of GATA in *IL-13* transcription, PT18 cells were transfected with pGL-705 or Mut 2, which are described above and in Fig. 2, along with various amounts of GATA-1 or -2 expression plasmids and stimulated with PMA/ionomycin. Mut2 showed mild reduction of GATA-binding potential but great reduction of AP-1-binding potential to the region between −106 and −94 in the *IL-13* promoter (Fig. 3*B*). As shown in Fig. 4*D*, GATA-1 and GATA-2 promoted *IL-13* transcription in a dose-dependent manner (pGL-705), but when mutations were introduced into the region between −106 and −94 in the *IL-13* promoter (Mut2), the transactivation of the *IL-13* gene by GATA proteins was abrogated. These findings indicate the possible involvement of AP-1 in *IL-13* transactivation by GATA.

Next, we transfected DN-c-*jun* into PT18 cells and evaluated the role of AP-1 in *IL-13* transactivation by GATA. As shown in Fig. 4*E*, DN-c-*jun* clearly inhibited the transactivation of pGL-106 by GATA proteins in PT18 cells. These findings indicate that AP-1 is indispensable for the transactivation of the *IL-13* gene induced by GATA proteins.

### *GATA-1 and GATA-2 associate with AP-1*

It has been reported that the cooperativeness between GATA-2 and AP-1 synergistically increases the transcriptional activity of the

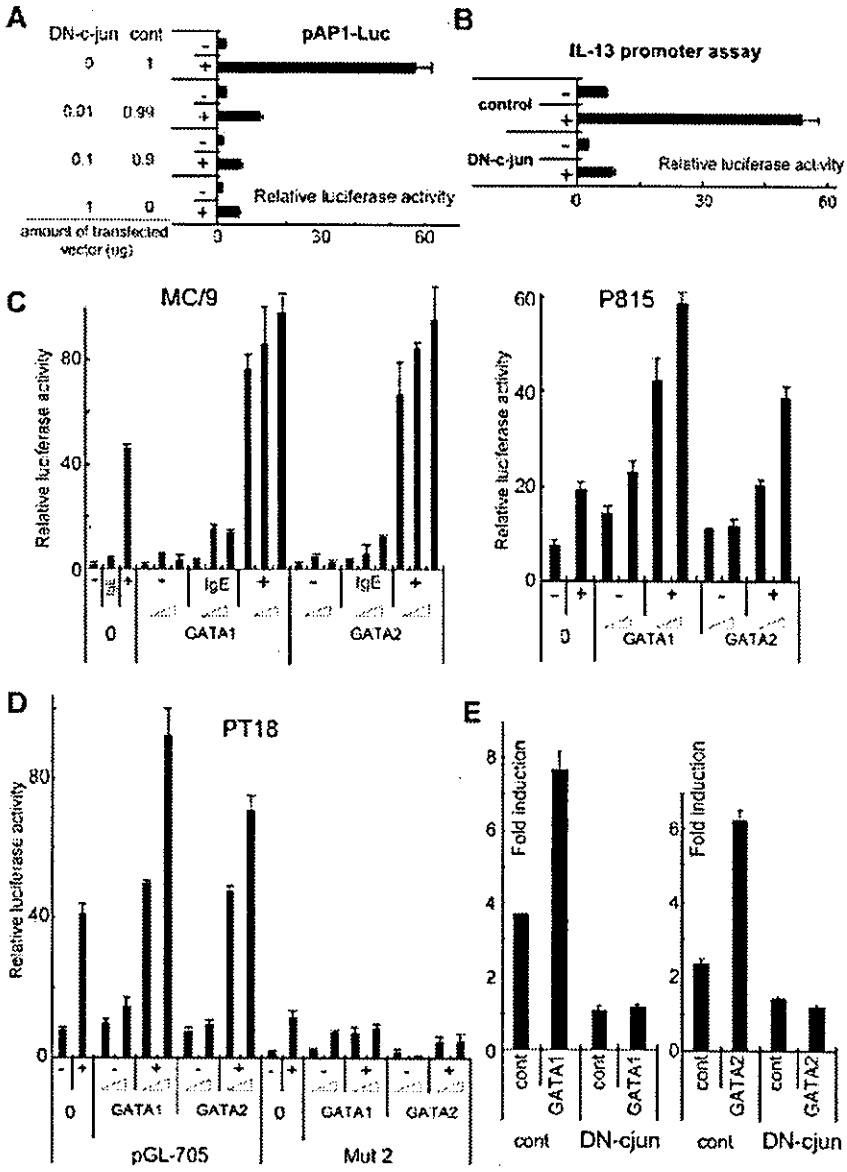


**FIGURE 4.** Both GATA-1 and GATA-2 transactivate the *IL-13* promoter through AP-1 activity. *A*, PT18 cells were transiently transfected with 1 μg of pAP1-luciferase plasmid, which is designed for monitoring induction of AP-1, and 0.1 μg of pRL/SV40 with the indicated dose of DN-c-*jun* expression plasmid or control plasmid (total 1 μg). Cells were stimulated with PMA/ionomycin for 12 h and luciferase activities were measured. *B*, PT18 cells were transiently transfected with 1 μg of pGL3–106 and 0.1 μg of pRL/SV40 with DN-c-*jun* expression plasmid or control plasmid (0.1 μg). Cells were stimulated with PMA/ionomycin for 12 h and luciferase activities were measured. *C*, MC/9 cells or P815 cells were transiently transfected with 1 μg of pGL3–106 and 0.1 μg of pRL/SV40 with an increasing dose of GATA-1 or -2 expression plasmid (0.01, 0.05, or 0.1 μg for MC/9 and 0.01 or 0.1 μg for P815 cells) or control plasmid. Cells were stimulated with PMA/ionomycin and luciferase activities were measured. *D*, PT18 cells were transiently transfected with 1 μg of *IL-13* promoter/luciferase plasmid (pGL3–705 or Mut2) and 0.1 μg of pRL/SV40 with an increasing dose (0.01 or 0.1 μg) of GATA-1 or -2 expression plasmid or control plasmid. Cells were stimulated PMA/ionomycin for 12 h and luciferase activities were measured. *E*, PT18 cells were transiently transfected with 1 μg of pGL3–106 and 0.1 μg of pRL/SV40 with DN-c-*jun* expression plasmid (0.1 μg), GATA expression plasmid (0.05 μg), or control plasmid. Cells were stimulated with PMA/ionomycin for 12 h and luciferase activities were measured. Units of luciferase activity were normalized based on values of pRL/SV40 activity for transfection activity (relative luciferase activity). The fold inductions were calculated as follows: (relative luciferase activity of stimulated cells)/(relative luciferase activity of unstimulated cells). A typical result of at least three independent experiments is shown.

endothelin-1 gene in endothelial cells (27). The authors demonstrated that GATA-2 and AP-1 bind into complexes in endothelial cells and HEK293 cells. However, the nature of this cooperativeness in the transcriptional activity of the *IL-13* promoter in mast cells has not been explored. Moreover, it is not clear whether GATA-1 interacts with AP-1. To elucidate these points, GATA-1 or GATA-2 N-terminally tagged with Myc, and c-*jun* N-terminally tagged with Flag were expressed in HEK293T cells, and immunoprecipitation analyses were performed. In this cell line, GATA proteins exist constitutively in the nucleus, whereas c-*jun* proteins translocate into the nucleus from the cytoplasm only after stimulation (data not shown). The cells were stimulated with PMA/ionomycin and nuclear lysates were harvested. As shown in Fig. 5*A*, we found that c-*jun* was coprecipitated with GATA-1 or GATA-2 after PMA/ionomycin stimulations.

We next examined these associations in mast cells by using a DNA-binding protein purification technique. By using magnetic particles to which oligonucleotides containing a DNA target sequence are coupled, the specific DNA-binding protein and associated proteins were harvested. In mast cells, GATA-1 and GATA-2 exist constitutively in the nucleus, whereas c-*fos* and c-*jun*, which are subunits of AP-1, translocate into the nucleus only after stimulation (Fig. 5*B*). As shown in Fig. 5*C*, by using particles coated with the oligonucleotides containing the sequence for the region between −108 and −94 in the IL-13 promoter, subunits of AP-1 and GATA-1 were efficiently purified from the nuclear lysate of PT18 cells stimulated with PMA/ionomycin. Next, we made particles coated with oligonucleotides containing the AP-1-specific binding sequence, and examined the association of GATA-1 with AP-1. As shown in Fig. 5*D*, GATA-1 was copurified with AP-1 and detected by Western blotting from the nuclear lysate of PT18 and MC/9 cells after various stimulations. Taken together, these findings clearly indicate that both GATA-1 and GATA-2 are capable of associating with AP-1.

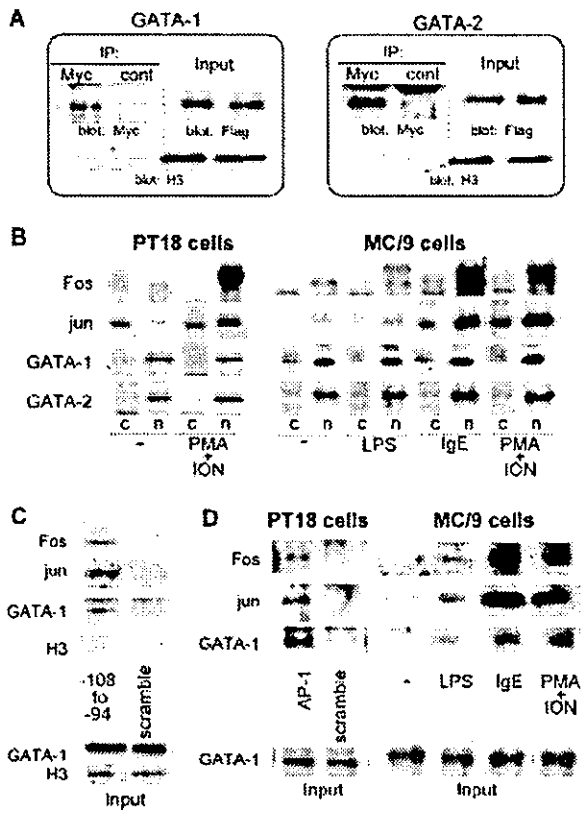


**FIGURE 5.** Both GATA-1 and GATA-2 associate with AP-1. *A*, HEK293T cells were transiently transfected with pEFBOS-Flag-c-*jun* (1 μg) in combination with either pEFBOS-Myc-GATA-1 or pEFBOS Myc-GATA-2 (1 μg). After 48 h, cells were stimulated with PMA/ionomycin for 15 min and nuclear extracts were prepared. Anti-Flag and control Ab immunoprecipitates were separated by SDS-PAGE, and immunoblotting was performed with anti-Flag Ab. Cell lysates were also probed with anti-Myc Ab (input) or anti-histone H3 Ab. As the m.w. of GATA-1 and GATA-2 is almost same as the Ig H chain, we could not evaluate the amount of immunoprecipitated GATA proteins. *B*, Distribution of GATA-1 and GATA-2 in mast cells. PT18 cells or MC/9 cells were stimulated with PMA/ionomycin, IgE cross-linking, or LPS for 15 min. Both nuclear extracts (n) and cytoplasmic lysates (c) were harvested, separated by SDS-PAGE, and immunoblottings were performed with the indicated Ab. *C*, PT18 cells were stimulated with PMA/ionomycin. Nuclear extracts harvested 15 min after stimulations were applied to the magnetic particle-ligated oligonucleotides containing the sequence for the region between −108 and −94 in the IL-13 promoter or scramble sequence. The purified proteins were eluted from the immobilized particle, separated by SDS-PAGE, and immunoblottings were performed with indicated Ab. Nuclear extracts were also probed with anti-GATA-1 or anti-histone H3 Ab (input). *D*, Nuclear extracts harvested 15 min after stimulations were applied to the magnetic particle-ligated oligonucleotides containing the sequence for AP-1-binding sequence (or scramble sequence in the case of PT18 cells). The purified proteins were eluted from the immobilized particle, separated by SDS-PAGE, and immunoblottings were performed with the indicated Ab. Nuclear extracts were also probed with anti-GATA-1 Ab (input).

### *GATA-1 interacts with AP-1 through its N-terminal region, C-terminal region, and N-finger domain*

To identify the AP-1-binding domain of GATA, we expressed several deletion mutants of GATA-1 in combination with Flag-tagged c-*jun* in HEK293T cells for coprecipitation assays. Although GATA proteins interact with other proteins through their N-terminal zinc finger or C-terminal zinc finger (16, 34), it has recently been reported that physical interaction is mediated through the N-terminal region or the C-terminal region of GATA (35). As shown in Fig. 6*A*, Flag-tagged c-*jun* was coprecipitated with all of the GATA deletion mutants: Δ1–86 (87–413), ΔN (194–413), ΔNF (1–199 and 249–413), ΔCF (1–251 and 287–413), and ΔC

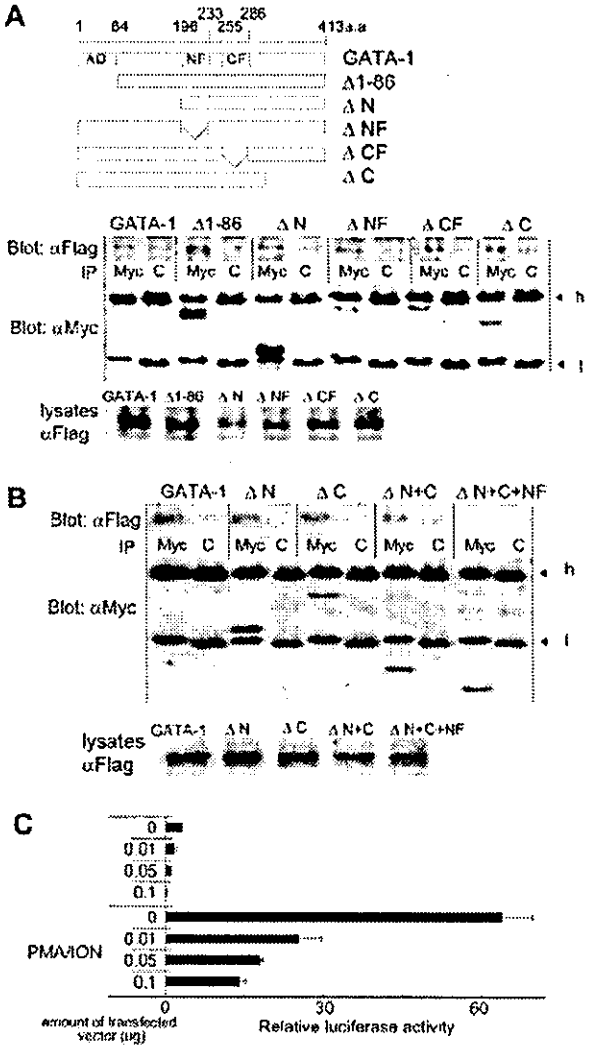


**FIGURE 6.** GATA-1 interacts with AP-1 through N-terminal, C-terminal, and N-finger domains. *A* and *B*, HEK 293T cells were transiently transfected with pEFBOS-Flag-c-*jun* (1 μg) in combination with the Myc-tagged GATA deletion mutant expression vector (1 μg). At 48 h after transfection, cells were stimulated with PMA/ionomycin for 15 min and nuclear extracts were prepared. Anti-Myc (Myc) and control (C) Ab immunoprecipitates were separated by SDS-PAGE, and immunoblotting was performed with anti-Flag Ab (*top panel*). The membrane was stripped and reprobed using anti-Myc Ab. Cell lysates were also probed with anti-Flag Ab. Arrows denote Ig H chain (h) or L chain (l). *C*, PT18 cells were transiently transfected with 1 μg of *IL-13* promoter/luciferase plasmid (pGL3–106) and 0.1 μg of pRL/SV40 with the indicated amount of GATA-1 deletion mutant expression plasmid (ΔC+ΔN+ΔNF). Cells were stimulated PMA/ionomycin for 12 h and luciferase activities were measured. Units of luciferase activity were normalized based on values of pRL/SV40 activity for transfection activity. A typical result of at least three independent experiments is shown.

(1–318). These results suggest that at least two domains of GATA-1 are required for the interaction with c-*jun*.

Next, we made two new deletion mutants of GATA-1, ΔN + C (194–318), and ΔN + C + NF (250–318), and expressed them in combination with the wild-type c-*jun* for coprecipitation assays in HEK293T cells. As shown in Fig. 6*B*, Flag-tagged c-*jun* was coprecipitated with ΔC, ΔN, and ΔN + C. However, no coprecipitation was detected for ΔN + C + NF, suggesting that all of these sites are essential for GATA-1 to associate with c-*jun*.

To confirm the importance of the interaction between GATA and c-*jun*, we transfected ΔN + C + NF in PT18 cells along with pGL-705 and performed luciferase assays. Transfection of this GATA deletion mutant reduced the transactivation of *IL-13* by PMA/ionomycin significantly (Fig. 6*C*). These results indicate the importance of the interaction between GATA and AP-1 in *IL-13* transcription.

*Overexpression of GATA-1 promotes IL-13 production in vivo*

To examine the ability of GATA-1 to promote the production of IL-13 in vivo, we transfected a Myc-tagged GATA-1 expression vector into P815 cells. Two clones stably expressing GATA-1 were isolated for analysis. As shown in Fig. 7*A*, one clone (designated 01) showed significant expression of Myc-tagged GATA-1, whereas the other clone (designated 02) showed only moderate expression. We then stimulated these cells with PMA/ionomycin and examined the production of IL-13 in culture supernatant. As shown in Fig. 7*B*, 01 cells showed significant IL-13 production and 02 cells showed moderate IL-13 production, whereas control cells produced much less IL-13.

To examine the importance of the interaction between GATA and AP-1 in vivo, ChIP experiments were performed using mast cell chromatin and Fos antisera. We confirmed that AP-1 binds to the IL-13 promoter after PMA/ionomycin stimulation in BMMCs (Fig. 7*C*). We then stimulated 01 and 02 cells with PMA/ionomycin and ChIP experiments were performed. As shown in Fig. 7*D*, 01 cells showed significant AP-1 binding to the *IL-13* promoter and control cells showed much less binding. The AP-1 binding levels exhibited the same tendency as the GATA-1 expression levels. These findings indicate the importance of GATA for the binding of AP-1 to the *IL-13* promoter. Based on these results, we concluded that the interaction between GATA and AP-1 promotes *IL-13* transcription and IL-13 production in vivo.

## Discussion

Almost nothing has been known about the regulation of *IL-13* transcription in mast cells, although we have previously reported that JNK is necessary for IL-13 transcription in mast cells stimulated by LPS (36). In T cells, the involvement of GATA-3 in cell type-specific expression of the *IL-13* gene has been reported (11). Moreover, GATA-3 seemed to transactivate the *IL-13* gene through its N-terminal region and N-finger domain in T cells (37). However, the mechanism that induces the transactivation of the *IL-13* gene immediately in response to stimulation has not been elucidated. Although rapid phosphorylation of GATA proteins other than GATA-3 after stimulations has been reported, its physiological significance is still controversial (12, 13). Furthermore, as shown in Figs. 3 and 5*B*, GATA-1 and GATA-2 constitutively exist in the nucleus and stimulation did not affect their DNA binding activity in mast cells. Taken together, these facts suggest that transcription factors other than GATA induce immediate transactivation of the *IL-13* gene in response to stimulation.

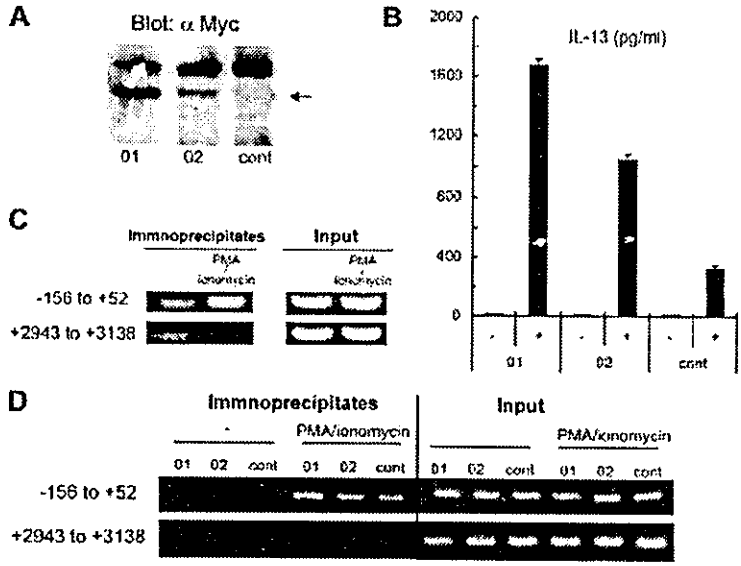


**FIGURE 7.** Overexpression of GATA-1 promotes IL-13 production in vivo. *A*, Expression of the Myc-tagged GATA-1 in P815 cells. Western blot analysis was performed with nuclear extracts from the G418-resistant clones transfected with the pEFBOS-Myc-GATA-1 vector along with pCDNA3 plasmid (01 or 02), or pCDNA3 alone (cont). An arrow denotes the band of Myc-tagged GATA-1. *B*, Cells ($2 \times 10^6$ cells/ml) were incubated in RPMI 1640 + 10% FCS with PMA/ionomycin (+) or not (−). The cell-free culture supernatants were collected after 24 h of culture. The IL-13 contents in the culture supernatants were assayed by ELISA using a mouse IL-13 ELISA system. The experiments were done in triplicate. The error bars represent SD values. *C*, Binding of AP-1 to the IL-13 promoter after PMA/ionomycin stimulation in BMMCs. *D*, The ability of AP-1 to bind to the *IL-13* promoter through interaction with GATA-1 in vivo. Cells were untreated or treated with PMA/ionomycin for 15 min. After treatment, chromatin was extracted and immunoprecipitated with anti-Fos Ab. PCR analyses of DNA products from immunoprecipitation reactions were conducted as described in *Materials and Methods*. PCR analyses were performed against the *IL-13* promoter region including the AP-1 binding site (−156 to +52) or downstream of the *IL-13* promoter (+2943 to +3138).

In the present study, we have shown that both AP-1 and GATA account for the transactivation of the *IL-13* gene and that AP-1 is indispensable for the transactivation of the *IL-13* gene induced by GATA proteins (Fig. 4). Furthermore, overexpression of GATA-1 induced a significant amount of IL-13 production and significant binding of AP-1 to the *IL-13* promoter (Fig. 7). These results indicate that activation of AP-1 is the key regulator of *IL-13* transcription and that GATA proteins promote the binding of AP-1 to the *IL-13* promoter in mast cells.

We have shown that GATA-1 and GATA-2 bind into complexes with AP-1 and that transfection of the deletion mutant of GATA-1 which results in the loss of association with c-*jun* (ΔN + C + NF) significantly reduced the transactivation of the *IL-13* gene in mast cells (Figs. 5 and 6). These results indicate the importance of physical interaction between GATA and AP-1 in *IL-13* transcription. However, recently it has been reported that both GATA-1 and GATA-2 regulate the histone acetylation pattern of chromatin, which is thought to improve the accessibility of other transcriptional factors (38, 39). Although the DNase hypersensitivity pattern of the *IL-13* gene in mast cells is unknown, it is possible that GATA proteins improve the binding of AP-1 to the *IL-13* promoter through modifying chromatin, in addition to direct interaction.

Various GATA-interacting proteins, including DNA-binding factors and general transcription activators and repressors, have been described (16). Most physical interactions are mediated by either the N-terminal zinc finger or the C-terminal zinc finger (16, 34). However, it has recently been reported that the N-terminal region (between residues 146 and 215) of GATA-3 interacts with smad-3 (35). Furthermore, it has quite recently been reported that the N-terminal region of GATA-4 interacts with c-*fos* (40). We have shown that GATA-1 interacts through its N-terminal, C-terminal, and N-finger domains with c-*jun* and that disruption of any single domain of GATA-1 dose not result in loss of the interaction with c-*jun*. Thus, GATA proteins interact with AP-1 through multiple domains. AP-1 consists of two subunits formed either by the heterodimerization of a Fos family protein with a Jun family protein or the homodimerization of Jun family members (41, 42). In the present study, although GATA and c-*jun* were overexpressed in HEK293T cells for the examination of the interaction between AP-1 and GATA, some overexpressed c-*jun* proteins probably bound endogenous Fos family proteins and acted as AP-1. In addition to direct binding, c-*jun* might bind to GATA proteins through Fos family proteins or other unknown proteins, and this might be the reason why GATA proteins interact with AP-1 through multiple domains.

The roles of AP-1 and GATA in Th2 cytokine production in T cells have been described in detail. P1, an element of the IL-4 promoter that binds AP-1, is important for Th2-restricted IL-4 expression (43). The IL-5 promoter has been shown to require both AP-1 and GATA elements for its activity in T cells (28). Among the GATA family proteins, GATA-3 plays a central role in Th2 cytokine production in T cells (9). Similarly to GATA-3, JunB, a component of AP-1, stimulates the expression of multiple Th2 cytokine genes (44). In mast cells, GATA-1 and GATA-2 play important roles in the transcription of both IL-4 and IL-5 (22, 23). Furthermore, the activation of JNK plays an important role in Th2 cytokine production in mast cells (36, 45), and it is well known that JNK activates AP-1 through the phosphorylation of c-*jun* (46). Similarly to GATA and AP-1, the NF-AT has been reported to play an important role in Th2 cytokine productions in mast cells. The transcription of IL-4 in mast cells is dependent on an NF-AT site in the murine IL-4 gene (47). The transcription of IL-5 in mast cells is also dependent on NF-AT (23). In the murine IL-13 promoter, there is an NF-AT-like binding site between −216 and −227 bp and, as shown in Fig. 1, a reduction of *IL-13* promoter activity was observed between pGL-322 and pGL-156. Furthermore, it has been reported that NF-AT acts in collaboration with both AP-1 and GATA (23, 48). In the present study, we have demonstrated that the interaction between AP-1 and GATA has a critical role in the production of IL-13 in mast cells. This interaction might play an essential role in Th2 cytokine production.

## Acknowledgments

We thank Dr. M. Yamamoto (Tsukuba University, Tsukuba, Japan) for helpful support and suggestions, Dr. N. Tsuboi (Nagoya University, Nagoya, Japan) for technical support, and Dr. K. Shimokata (Nagoya University, Nagoya, Japan) for review of the manuscript.

## References

1. Cherwinski, H. M., J. H. Schumacher, K. D. Brown, and T. R. Mosmann. 1987. Two types of mouse helper T cell clone. III. Further differences in lymphokine synthesis between Th1 and Th2 clones revealed by RNA hybridization, functionally monospecific bioassays, and monoclonal antibodies. *J. Exp. Med. 166:1229.*
2. Brown, K. D., S. M. Zurawski, T. R. Mosmann, and G. Zurawski. 1989. A family of small inducible proteins secreted by leukocytes are members of a new superfamily that includes leukocyte and fibroblast-derived inflammatory agents, growth factors, and indicators of various activation processes. *J. Immunol. 142:679.*
3. McKenzie, A. N., J. A. Culpepper, R. de Waal Malefyt, F. Briere, J. Punnonen, G. Aversa, A. Sato, W. Dang, B. G. Cocks, S. Menon, et al. 1993. Interleukin 13, a T-cell-derived cytokine that regulates human monocyte and B-cell function. *Proc. Natl. Acad. Sci. USA 90:3735.*
4. Burd, P. R., W. C. Thompson, E. E. Max, and F. C. Mills. 1995. Activated mast cells produce interleukin 13. *J. Exp. Med. 181:1373.*
5. Zurawski, G., and J. E. de Vries. 1994. Interleukin 13, an interleukin 4-like cytokine that acts on monocytes and B cells, but not on T cells. *Immunol. Today 15:19.*
6. Wills-Karp, M., J. Luyimbazi, X. Xu, B. Schofield, T. Y. Neben, C. L. Karp, and D. D. Donaldson. 1998. Interleukin-13: central mediator of allergic asthma. *Science 282:2258.*
7. Grunig, G., M. Warnock, A. E. Wakil, R. Venkayya, F. Brombacher, D. M. Rennick, D. Sheppard, M. Mohrs, D. D. Donaldson, R. M. Locksley, and D. B. Corry. 1998. Requirement for IL-13 independently of IL-4 in experimental asthma. *Science 282:2261.*
8. Hershey, G. K. 2003. IL-13 receptors and signaling pathways: an evolving web. *J. Allergy Clin. Immunol. 111:677.*
9. Zhou, M., and W. Ouyang. 2003. The function role of GATA-3 in Th1 and Th2 differentiation. *Immunol. Res. 28:25.*
10. Takemoto, N., Y. Kamogawa, H. Jun Lee, H. Kurata, K. I. Arai, A. O'Garra, N. Arai, and S. Miyatake. 2000. Cutting edge: chromatin remodeling at the IL-4/IL-13 intergenic regulatory region for Th2-specific cytokine gene cluster. *J. Immunol. 165:6687.*
11. Kishikawa, H., J. Sun, A. Choi, S. C. Miaw, and I. C. Ho. 2001. The cell type-specific expression of the murine IL-13 gene is regulated by GATA-3. *J. Immunol. 167:4414.*
12. Crossley, M., and S. H. Orkin. 1994. Phosphorylation of the erythroid transcription factor GATA-1. *J. Biol. Chem. 269:16589.*
13. Tremblay, J. J., and R. S. Viger. 2003. Transcription factor GATA-4 is activated by phosphorylation of serine 261 via the cAMP/protein kinase a signaling pathway in gonadal cells. *J. Biol. Chem. 278:22128.*
14. Zon, L. I., M. F. Gurish, R. L. Stevens, C. Mather, D. S. Reynolds, K. F. Austen, and S. H. Orkin. 1991. GATA-binding transcription factors in mast cells regulate the promoter of the mast cell carboxypeptidase A gene. *J. Biol. Chem. 266:22948.*
15. Harigae, H., S. Takahashi, N. Suwabe, H. Ohtsu, L. Gu, Z. Yang, F. Y. Tsai, Y. Kitamura, J. D. Engel, and M. Yamamoto. 1998. Differential roles of GATA-1 and GATA-2 in growth and differentiation of mast cells. *Genes Cells 3:39.*
16. Molkentin, J. D. 2000. The zinc finger-containing transcription factors GATA-4, -5, and -6: ubiquitously expressed regulators of tissue-specific gene expression. *J. Biol. Chem. 275:38949.*
17. Orkin, S. H. 1998. Embryonic stem cells and transgenic mice in the study of hematopoiesis. *Int. J. Dev. Biol. 42:927.*
18. Martin, D. I., L. I. Zon, G. Mutter, and S. H. Orkin. 1990. Expression of an erythroid transcription factor in megakaryocytic and mast cell lineages. *Nature 344:444.*
19. Bocek, P., Jr., M. D. Guthmann, and I. Pecht. 1997. Analysis of the genes encoding the mast cell function-associated antigen and its alternatively spliced transcripts. *J. Immunol. 158:3235.*
20. Maeda, K., C. Nishiyama, T. Tokura, Y. Akizawa, M. Nishiyama, H. Ogawa, K. Okumura, and C. Ra. 2003. Regulation of cell type-specific mouse FcεRI β-chain gene expression by GATA-1 via four GATA motifs in the promoter. *J. Immunol. 170:334.*
21. Nishiyama, C., T. Yokota, K. Okumura, and C. Ra. 1999. The transcription factors Elf-1 and GATA-1 bind to cell-specific enhancer elements of human high-affinity IgE receptor α-chain gene. *J. Immunol. 163:623.*

22. Hural, J. A., M. Kwan, G. Henkel, M. B. Hock, and M. A. Brown. 2000. An intron transcriptional enhancer element regulates IL-4 gene locus accessibility in mast cells. *J. Immunol. 165:3239.*
23. Prieschl, E. E., V. Gouilleux-Gruart, C. Walker, N. E. Harrer, and T. Baumruker. 1995. A nuclear factor of activated T cell-like transcription factor in mast cells is involved in IL-5 gene regulation after IgE plus antigen stimulation. *J. Immunol. 154:6112.*
24. Ney, P. A., B. P. Sorrentino, K. T. McDonagh, and A. W. Nienhuis. 1990. Tandem AP-1-binding sites within the human β-globin dominant control region function as an inducible enhancer in erythroid cells. *Genes Dev. 4:993.*
25. Walters, M., and D. I. Martin. 1992. Functional erythroid promoters created by interaction of the transcription factor GATA-1 with CACCC and AP-1/NFE-2 elements. *Proc. Natl. Acad. Sci. USA 89:10444.*
26. Lee, M. E., M. S. Dhadly, D. H. Temizer, J. A. Clifford, M. Yoshizumi, and T. Quertermous. 1991. Regulation of endothelin-1 gene expression by Fos and Jun. *J. Biol. Chem. 266:19034.*
27. Kawana, M., M. E. Lee, E. E. Quertermous, and T. Quertermous. 1995. Cooperative interaction of GATA-2 and AP1 regulates transcription of the endothelin-1 gene. *Mol. Cell. Biol. 15:4225.*
28. Yamagata, T., J. Nishida, R. Sakai, T. Tanaka, H. Honda, N. Hirano, H. Mano, Y. Yazaki, and H. Hirai. 1995. Of the GATA-binding proteins, only GATA-4 selectively regulates the human interleukin-5 gene promoter in interleukin-5-producing cells which express multiple GATA-binding proteins. *Mol. Cell. Biol. 15:3830.*
29. Masuda, A., T. Matsuguchi, K. Yamaki, T. Hayakawa, M. Kubo, W. J. LaRochelle, and Y. Yoshikai. 2000. Interleukin-15 induces rapid tyrosine phosphorylation of STAT6 and the expression of interleukin-4 in mouse mast cells. *J. Biol. Chem. 275: 29331.*
30. Adachi, O., T. Kawai, K. Takeda, M. Matsumoto, H. Tsutsui, M. Sakagami, K. Nakanishi, and S. Akira. 1998. Targeted disruption of the MyD88 gene results in loss of IL-1- and IL-18-mediated function. *Immunity 9:143.*
31. Matsuguchi, T., T. Musikacharoen, T. R. Johnson, A. S. Kraft, and Y. Yoshikai. 2001. A novel mitogen-activated protein kinase phosphatase is an important negative regulator of lipopolysaccharide-mediated c-Jun N-terminal kinase activation in mouse macrophage cell lines. *Mol. Cell. Biol. 21:6999.*
32. Musikacharoen, T., Y. Yoshikai, and T. Matsuguchi. 2003. Histone acetylation and activation of cAMP-response element-binding protein regulate transcriptional activation of MKP-M in lipopolysaccharide-stimulated macrophages. *J. Biol. Chem. 278:9167.*
33. Peakman, M. C., C. Colby, L. I. Perrotti, P. Tekumalla, T. Carle, P. Ulery, J. Chao, C. Duman, C. Steffen, L. Monteggia, et al. 2003. Inducible, brain region-specific expression of a dominant negative mutant of c-Jun in transgenic mice decreases sensitivity to cocaine. *Brain Res. 970:73.*
34. Crispino, J. D., M. B. Lodish, J. P. MacKay, and S. H. Orkin. 1999. Use of altered specificity mutants to probe a specific protein-protein interaction in differentiation: the GATA-1:FOG complex. *Mol. Cell 3:219.*
35. Blokzijl, A., P. ten Dijke, and C. F. Ibanez. 2002. Physical and functional interaction between GATA-3 and Smad3 allows TGF-β regulation of GATA target genes. *Curr. Biol. 12:35.*
36. Masuda, A., Y. Yoshikai, K. Aiba, and T. Matsuguchi. 2002. Th2 cytokine production from mast cells is directly induced by lipopolysaccharide and distinctly regulated by c-Jun N-terminal kinase and p38 pathways. *J. Immunol. 169:3801.*
37. Takemoto, N., K. Arai, and S. Miyatake. 2002. Cutting edge: the differential involvement of the N-finger of GATA-3 in chromatin remodeling and transactivation during Th2 development. *J. Immunol. 169:4103.*
38. Letting, D. L., C. Rakowski, M. J. Weiss, and G. A. Blobel. 2003. Formation of a tissue-specific histone acetylation pattern by the hematopoietic transcription factor GATA-1. *Mol. Cell. Biol. 23:1334.*
39. Ozawa, Y., M. Towatari, S. Tsuzuki, F. Hayakawa, T. Maeda, Y. Miyata, M. Tanimoto, and H. Saito. 2001. Histone deacetylase 3 associates with and represses the transcription factor GATA-2. *Blood 98:2116.*
40. McBride, K., F. Charron, C. Lefebvre, and M. Nemer. 2003. Interaction with GATA transcription factors provides a mechanism for cell-specific effects of c-Fos. *Oncogene 22:8403.*
41. Angel, P., and M. Karin. 1991. The role of Jun, Fos and the AP-1 complex in cell-proliferation and transformation. *Biochim. Biophys. Acta 1072:129.*
42. D'Alonzo, R. C., N. Selvamurugan, G. Karsenty, and N. C. Partridge. 2002. Physical interaction of the activator protein-1 factors c-Fos and c-Jun with Cbfa1 for collagenase-3 promoter activation. *J. Biol. Chem. 277:816.*
43. Rooney, J. W., T. Hoey, and L. H. Glimcher. 1995. Coordinate and cooperative roles for NF-AT and AP-1 in the regulation of the murine IL-4 gene. *Immunity 2:473.*
44. Li, B., C. Tournier, R. J. Davis, and R. A. Flavell. 1999. Regulation of IL-4 expression by the transcription factor JunB during T helper cell differentiation. *EMBO J. 18:420.*
45. Garrington, T. P., T. Ishizuka, P. J. Papst, K. Chayama, S. Webb, T. Yujiri, W. Sun, S. Sather, D. M. Russell, S. B. Gibson, et al. 2000. MEKK2 gene disruption causes loss of cytokine production in response to IgE and c-Kit ligand stimulation of ES cell-derived mast cells. *EMBO J. 19:5387.*
46. Johnson, G. L., and R. Lapadat. 2002. Mitogen-activated protein kinase pathways mediated by ERK, JNK, and p38 protein kinases. *Science 298:1911.*
47. Weiss, D. L., J. Hural, D. Tara, L. A. Timmerman, G. Henkel, and M. A. Brown. 1996. Nuclear factor of activated T cells is associated with a mast cell interleukin 4 transcription complex. *Mol. Cell. Biol. 16:228.*
48. Macian, F., C. Lopez-Rodriguez, and A. Rao. 2001. Partners in transcription: NFAT and AP-1. *Oncogene 20:2476.*

# Interleukin-15 induces IL-12 receptor β1 gene expression through PU.1 and IRF 3 by targeting chromatin remodeling

Tipayaratn Musikacharoen, Asako Oguma, Yasunobu Yoshikai, Norika Chiba, Akio Masuda, and Tetsuya Matsuguchi

**Interleukin-12 receptor β1 (IL12RB1) is expressed on a variety of immune cells, including T and natural killer (NK) cells and macrophages, and is involved in innate and adaptive immune responses. Levels of IL12RB1 mRNA are dynamically regulated by various cytokines, including interferon-γ (IFN-γ) and IL-15. To reveal the regulatory mechanisms governing IL12RB1 gene expression, we analyzed the transcriptional regulatory region of the mouse IL12RB1 gene. Promoter analyses in a mouse macrophage cell line, RAW264.7, revealed that the 2508-bp region upstream of the transcriptional start site is sufficient for the full transcriptional activation of the IL12RB1 gene by IFN-γ or IL-15. Analyses of the deletion mutants revealed critical roles of IRE/ISRE and ETS/PU.1 elements, to which IRF3 and PU.1, respectively, bound. Notably, chromatin immunoprecipitation (ChIP) assays revealed IL-15 rapidly induced histone H3 acetylation at the IL12RB1 promoter. Consistently, IL-15, as a histone deacetylase inhibitor, synergistically enhanced IL12RB1 gene expression and promoter activation by IFN-γ through increased protein binding to ETS/PU.1 and IRE/ISRE sites. Additionally, IL12RB1 promoter activation by IFN-γ was enhanced by the coexpression of a coactivator protein, CBP. Thus, IL-15 induces chromatin remodeling of the IL12RB1 gene promoter, increasing IL12RB1 mRNA expression in synergy with IFN-γ through the recruitment of PU.1 and IRF3. (Blood. 2005;105:711-720)**



## Introduction

Interleukin-12 (IL-12) is a cytokine predominantly produced by antigen-presenting cells (APCs), such as dendritic cells (DCs) and macrophages, in response to various infectious agents, and it is essential for the development of efficient innate and T-helper 1 ($T_H1$)—type adaptive immunity. The distinctive role of IL-12 is to induce interferon-γ (IFN-γ) production by natural killer (NK) and T cells in response to a variety of inflammatory stimuli.[1] IFN-γ in turn activates macrophages to express numerous genes associated with inflammatory responses, including IFN-γ production itself.[1,2] Several recent studies, however, revealed that IL-12 also stimulates DCs and macrophages in autocrine and paracrine manners to produce abundant amounts of IFN-γ.[3-5]

IL-12 receptor (IL-12R) is composed of 2 subunits, β1 and β2,[6,7] each of which belongs to the cytokine receptor superfamily and is highly homologous to gp130, granulocyte–colony-stimulating factor receptor (G-CSF-R), and leukemia inhibitory factor–receptor (LIF-R).[8] Although IL12RB1 and IL-12Rβ2 share a similar structure, their binding affinities are distinct. In humans, IL12RB1 and IL-12Rβ2 separately bind IL-12 with low affinity, but together they bind IL-12 with high affinity.[9] In mice, IL-12Rβ2 binds IL-12 at very low affinity, whereas IL12RB1 binds with low and high affinities.[10] Genetic deficiency of IL12RB1 causes severe infection by low-pathogen bacteria, such as bacilli Calmette-Guerin (BCG), in humans and in mice, most likely because of insufficient IFN-γ production,[7,11,12] indicating that IL12RB1 is essential for the host defense mechanisms. It has recently been reported that IL12RB1 is also a component of the receptor complex for another IFN-γ–inducing cytokine, IL-23.[13]

IL12RB1 expression is under dynamic regulation in response to various stimuli. In vivo, IL12RB1 mRNA levels in macrophages are increased by IL-12 as a consequence of IFN-γ expression.[14] Consequently, direct stimulation of macrophages by IFN-γ upregulated IL12RB1 mRNA.[15] In peripheral blood mononuclear cells (PBMCs), IL12RB1 gene expression is induced by phytohemagglutinin (PHA), anti-CD3/CD28 monoclonal antibody (mAb), IL-2, IL-7, and IL-15 stimulation.[16]

IL-15 receptor is composed of the specific IL-15Rα and 2 receptor chains, IL-2Rβ and IL-2Rγc, which are shared by IL-2. Although IL-2Rα is predominantly expressed on activated T cells, IL-15Rα has been identified in multiple cell types, including APCs.[17] Notably, the lipopolysaccharide (LPS)–induced IFN-γ response in severe combined immune deficient (SCID) mice was significantly reduced by pretreatment with a neutralizing anti–IL-15 antibody, indicating IL-15 participates in IFN-γ induction in a T cell–independent fashion.[18] Moreover, splenic DCs and peritoneal macrophages from IL-$15^{-/-}$ mice produced significantly less IFN-γ than their control counterparts in response to IL-12, suggesting IL-12 controls IFN-γ production by APCs in an IL-15–dependent manner.[19] This appeared to be caused by the essential role of IL-15 in IL12RB1 expression in APCs, because

From the Division of Biochemistry and Molecular Dentistry, Department of Developmental Medicine, Kagoshima University, Graduate School of Medical and Dental Sciences, Kagoshima; Division of Host Defense, Center for Neural Disease and Cancer, Nagoya University Graduate School of Medicine; and Division of Host Defense, Research Center of Prevention of Infectious Diseases, Medical Institute of Bioregulation, Kyushu University, Japan.

Submitted March 5, 2004; accepted August 26, 2004. Prepublished online as *Blood* First Edition Paper, September 2, 2004; DOI 10.1182/blood-2004-03-0842.

Supported in part by grants from the Ministry of Education, Science and Culture of the Japanese Government, the Yakult Bioscience Foundation, the Ohyama Health Foundation, and the Japan Society for the Promotion of Science.

**Reprints:** T. Matsuguchi, Division of Biochemistry and Molecular Dentistry, Department of Developmental Medicine, Kagoshima University, Graduate School of Medical and Dental Sciences, 8-35-1 Sakuragaoka, Kagoshima, Japan; e-mail: tmatsugu@denta.hal.kagoshima-u.ac.jp.

The publication costs of this article were defrayed in part by page charge payment. Therefore, and solely to indicate this fact, this article is hereby marked "advertisement" in accordance with 18 U.S.C. section 1734.

IL12RB1 mRNA expression is significantly reduced in APCs from IL-15, $\gamma c^{-/-}$, RAG-$2^{-/-}$, and IL-2R$\beta^{-/-}$RAG-$2^{-/-}$ mice.[19] These lines of evidence indicated that IL-15–mediated IL12RB1 expression on APCs is important in the generation of $T_H1$-type immune responses.

Thus, IL12RB1 mRNA expression in APCs is regulated by IFN-γ and IL-15, but the molecular mechanisms governing IL-12Rβ1 transcription have not been extensively studied. In this study, we isolated mouse IL12RB1 genomic clones and investigated the transcriptional regulation in a mouse macrophage cell line. We here show that IL-15 and IFN-γ synergistically activated IL12RB1 gene expression through the cooperation of 2 transcription factors, PU.1 and IRF3. IL12RB1 gene transcription is also associated with histone acetylation and chromatin remodeling of the gene, which are efficiently induced by IL-15.

## Materials and methods

### Antibodies and reagents

Recombinant mouse IFN-γ and IL-15 were purchased from Peprotech (Seattle, WA). Anti–phospho-histone H3 (Ser 10), anti–acetyl-histone H3, and anti–acetyl-histone H4 antibodies were purchased from Upstate Biotechnology (Lake Placid, NY). Antihemagglutinin (HA), anti-p38, anti-JNK1, anti-PU.1, and anti-IRF3 antibodies were obtained from Santa Cruz Biotechnology (Santa Cruz, CA). Phosphospecific anti-p38, anti-JNK, and antiphosphoserine antibodies were purchased from New England Biolabs (Beverly, MA). Lipopolysaccharide (LPS) from *Escherichia coli* serotype B5 055 and trichostatin A (TSA) were obtained from Sigma Chemical (St Louis, MO). Specific mitogen-activated protein kinase (MAPK) inhibitors SB203580 and SP600125 were purchased from Calbiochem (San Diego, CA).

### Isolation and characterization of the mouse IL12RB1 genomic clones

The mouse IL12RB1 cDNA containing the 5′ portion of the coding region was prepared by reverse transcription–polymerase chain reaction (RT-PCR) using 2 primers, (5′-CTGCAGAAGTTCCTGGGGCCT and 5′-CCCGGGCAGGTGCTCAGCTG), from the total RNA of RAW264.7 cells, and was used for screening the mouse genomic phage library in Lambda Fix II (Stratagene, La Jolla, CA), as previously described.[20]

### Primer extension analysis

Total RNA was prepared from IFN-γ–stimulated RAW264.7 cells. Contaminating DNA was removed by treatment with 10 μg/mL DNase I (Sigma) for 2 hours at 16°C. Remaining RNA was extracted twice with phenol/chloroform and was subjected to poly $(A)^+$ RNA purification using the mRNA purification kit (Amersham Biosciences, Piscataway, NJ). An oligonucleotide, 5′-CCCATCATGTCCATGAGGAGCCGAGTCGTG, complementary to the 5′ untranslated region of the IL12RB1 cDNA (GenBank/EMBL accession number NM 008353) was 5′ end-labeled with $^{32}P$. Annealing of the labeled primer to poly $(A)^+$ RNA was performed in 11 μL of 2 × first-strand buffer (Invitrogen, Carlsbad, CA) by heating the mixture of 2 pmol labeled primer and 10 μg poly $(A)^+$ RNA at 48°C for 40 minutes and by cooling to room temperature for 20 minutes. Reverse transcription was run on a 6% denaturing polyacrylamide urea gel, as previously described.[21]

### Generation of the mouse IL12RB1 promoter constructs

A series of sense oligonucleotides—AGATCTGTGTTCCTGCAGAG (pGL3-3875), GGAATGTTAACCTGCGAGTG (pGL3-2508), ACTCCCTTGATTGGGCCACC (pGL3-1803), TAGGCAGGCCCCCCAGCCTG (pGL3-1483), CAGGACACTTGACCCCTGGG (pGL3-849), AGGGCCATATCGTATCTGTG (NF-κB del), TTGGTTTCCCAAAGCCGCCT (ETS/PU.1 del), CATGCAGCCTTTGCTCTGTG (IRE/ISRE del)—and an antisense oligonucleotide—CCAGGAACTTCTGCAGGGCTG—were used to generate a series of 5′ deletion DNA fragments. The PCR products were digested with *KpnI*/*MluI* (pGL3-3875) or *XhoI*/*MluI* (all the others) and was subcloned into the pGL3-basic vector (Promega). To generate the IRE/ISRE-mutated construct, 2 PCR products from 2 pairs of primers (GGAATGTTAACCTGCGAGTG and GCAGATGGGTTTTCAGACAG; CATGCAGCCTTTGCTCTCGT and CCAGGAACTTCTGCAGGGCTG) were amplified, digested with *EcoRI*, ligated, and cloned into the pGL3-basic vector. The mammalian expression plasmid pcDNA3-CBP-HA was a kind gift from Dr R Eckner (Institute for Molecular Biology, Zurich, Switzerland).[22]

### Transfection and luciferase assays

A mouse macrophage cell line, RAW264.7, was obtained from RIKEN cell bank (Tsukuba, Japan). RAW264.7 stable transfectants were generated as previously described.[23] For luciferase assays, cells were plated onto 35-mm plate at $1 \times 10^5$ cells/plate. Twenty-four hours after plating, cells were supplied with Dulbecco modified Eagle medium (DMEM) plus 1% fetal calf serum (FCS) and were left untreated or were treated with 10 ng/mL IFN-γ, 10 ng/mL IL-15, 1 μg/mL LPS, 100 nM TSA, or their combination for 8 hours. Luciferase activity in the cell lysates was measured using a single luciferase assay system (Promega) according to the manufacturer's instructions. All luciferase assays shown in the current study were performed in triplicate, and the average of 3 independent experiments was shown.

### Northern blot analysis

Northern blotting was performed as previously described.[23] For the probes, cDNA fragments containing the full coding regions of mouse IL12RB1, IRF1, IRF2, IRF3, and IRF7 were prepared by RT-PCR from total RNA of IFN-γ–treated RAW264.7 cells and were $^{32}P$-labeled with the Prime-a-Gene labeling kit (Promega).

### EMSA

Nuclear extracts were prepared from RAW264.7 cells as previously described.[24,25] Primers used for electrophoretic mobility shift assay (EMSA) were 5′-TGGACTTCCC for NF-κB, 5′-GGTAGAGGAAGTCCAG for ETS/PU.1, 5′-AAAAAACTCAAACTG for IRE/ISRE, 5′-TTATTGATAACTGG for GATA1, 5′-TGTTCCTTGAAAACT for STAT/STAT5, and 5′-CACACGTGT for E-Box/USF. Approximately $1 \times 10^5$ cpm of an oligonucleotide, radiolabeled by $\gamma^{32}P$-ATP with T4 polynucleotide kinase, 2 μg nuclear extracts, and 1 μg poly (dI-dC), was added to the binding buffer (20 mM HEPES [*N*-2-hydroxyethylpiperazine-*N*′-2-ethanesulfonic acid]–KOH [pH 7.9], 60 mM KCl, 1 mM dithiothreitol [DTT], 1 mM EDTA [ethylenediaminetetraacetic acid], and 5% glycerol)[26] and was incubated for 30 minutes at 4°C. Specific IRF blockers used for the competition assays were C13 5′-AAGTGAAAGTGAAAGTGA for IRF1/IRF2,[27] PRDIII 5′-GAAAACTGAAAGGG for IRF3, and 5′ GAAAGTGAACGC for IRF7.[28] The mutated primer for IRF3/IRF7, 5′-GAAAGTCTTCGC,[28] was used as a negative control. Competition assays were performed by incubating nuclear extracts with a 5- or a 50-fold excess of unlabeled oligonucleotide before the addition of the $^{32}P$-labeled probe. For supershift assays, 2 μg anti-PU.1 or anti-IRF3 antibody was preincubated with nuclear extracts for 1 hour. Reaction mixtures were run through a 6% nondenaturing polyacrylamide gel at 4°C in TBE buffer.

### Immunoblotting and immunoprecipitation

Total cellular lysate preparation, Western blotting, and immunoprecipitation were performed as previously described.[23]

### Chromatin immunoprecipitation assay

Acetyl-histone chromatin immunoprecipitation (ChIP) assay was performed according to the manufacturer's instruction (Upstate Biotechnology). After IFN-γ, IL-15, or LPS stimulation, chromatin cross-linking, immunoprecipitation, and PCR amplification were performed essentially as

previously described.[21] The IL12RB1 promoter-specific primers were: sense, CATATGGTATCTGTGTGTTT; antisense, ACGAGAGCAAAG-GCTGCATG. The locations of these primers are indicated in Figure 2C. PCR amplifies the genomic region containing ETS/PU.1 and IRE/ISRE consensus sites. PCR conditions were as follows: 94°C for 3 minutes; 20 to 25 cycles at 94°C for 30 seconds and at 66°C for 2 minutes; 72°C for 7 minutes, followed by 3 cycles with the $\gamma^{32}$P-ATP–labeled antisense primer. PCR products were analyzed by electrophoresis on a 6% denaturing polyacrylamide gel. For each reaction, 1% of the cross-link–released chromatin was saved and used as an input control.

## Results

### IL12RB1 gene expression in RAW264.7 cells

As a model for APCs expressing IL12RB1, we analyzed a commonly used mouse macrophage cell line, RAW264.7. To reveal the expression pattern of IL12RB1 mRNA, cells were left untreated or were stimulated with LPS, IL-15, or IFN-γ for 4 hours, and total RNAs were subjected to Northern blot analyses. As shown in Figure 1A, a small amount of IL12RB1 mRNA was constitutively expressed in untreated RAW264.7 cells. Stimulation of the cells with IFN-γ or IL-15 (10 ng/mL each) significantly increased IL12RB1 gene expression, whereas no remarkable change was detected after LPS stimulation even at concentrations as high as 1 μg/mL.

### Isolation of mouse IL12RB1 genomic DNA containing 5′ promoter region

To identify the transcriptional regulatory region of the mouse IL12RB1 gene, we screened a mouse genomic library with an IL12RB1 cDNA probe. A 15-kb fragment of the IL12RB1 genomic DNA, which appeared to include approximately 4.5 kb of the putative 5′ flanking region, was isolated (Figure 1C). Primer extension analysis was then carried out to map the transcriptional start site. A synthetic oligonucleotide complementary to the 5′ end region of the reported IL12RB1 cDNA (GenBank/EMBL accession number NM 008353) was hybridized to poly (A)$^+$ RNA from IFN-γ–stimulated RAW264.7 cells and was extended by reverse transcription. As shown in Figure 1B, the analysis revealed a major transcriptional start site (indicated as 1) and 2 minor sites (indicated as 2 and 3). The proximal major transcriptional start site (1) was located at 87 bp upstream from the 5′ end of the previously described cDNA sequence (GenBank/EMBL accession number NM 008353), and the nucleotide of this site (T) was designed as +1 throughout this report. The second and third minor transcriptional start sites were 7 and 30 bp upstream of the first major site, respectively. The schematic presentation of the mouse IL12RB1 gene structure is shown in Figure 1C.

### Identification of the regulatory elements involved in IL12RB1 gene transcription

The nucleotide sequence upstream of the transcriptional start sites was searched for the potential binding sites for transcription factors using Genome Exploring and Modeling Software.[29] Neither TATA nor CAAT boxes were present in the 5′ upstream region of each of the 3 transcriptional start sites. A series of 5′ deletion luciferase constructs (Figure 2A) was initially generated to locate the region required for IL12RB1 gene transcription. The generated plasmids were stably integrated into RAW264.7 cells, and several independent clones for each construct were isolated for stimulation with IFN-γ, IL-15, or LPS. Among the reporter constructs, the highest fold induction by IFN-γ or IL-15 was obtained from the longest pGL3-3875 construct, but no significant decrease was detected with the pGL3-2508 construct, indicating the 2508-bp region is sufficient for the full transcriptional activation of the IL12RB1 gene by these 2 cytokines. Further deletion to −1803 (pGL3-1803) completely abrogated promoter responsiveness to IFN-γ or

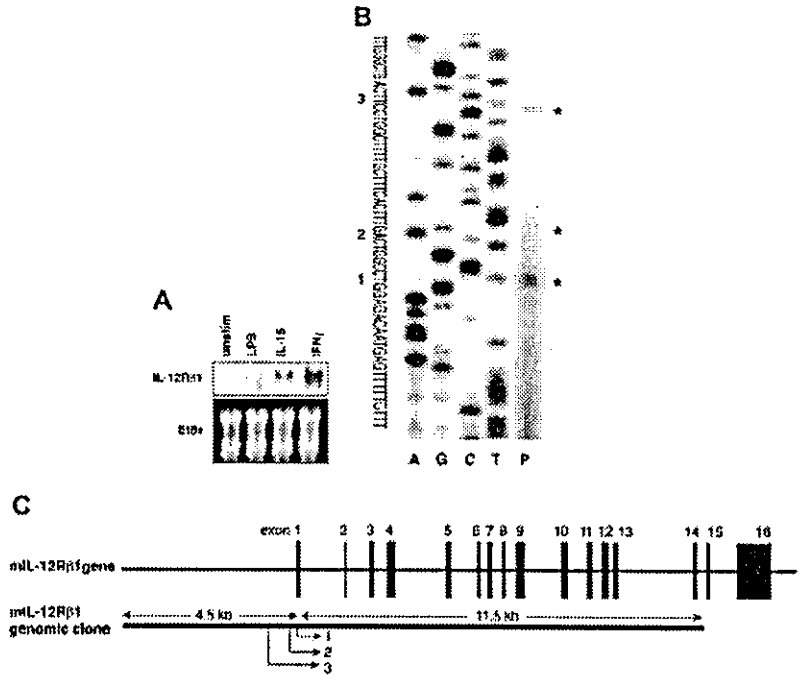


**Figure 1. Expression and molecular cloning of the mouse IL12RB1 gene.** (A) IL-15 and IFN-γ, but not LPS, induce IL12RB1 gene expression in a mouse macrophage cell line. RAW264.7 cells were left untreated (unstim) or treated for 4 hours with 1 μg/mL LPS, 10 ng/mL IL-15, or 10 ng/mL IFN-γ. Total RNA (20 μg each) was prepared for the Northern blot analysis using a $^{32}$P-labeled IL12RB1 cDNA probe. Gene expression of IL12RB1 and a picture of the ethidium bromide (EtBr)–stained gel are shown. (B) Transcription start sites of the IL12RB1 gene were mapped by primer extension analysis. The transcribed product (P) was run along with sequencing ladder from the same primer on a 6% polyacrylamide/urea gel. Asterisks indicate the transcribed products; 3 transcriptional start sites are shown, and the proximal major site was designed as +1. (C) Schematic presentation of the mouse IL12RB1 gene. Black boxes represent exons. Positions of 3 transcriptional start sites are indicated.

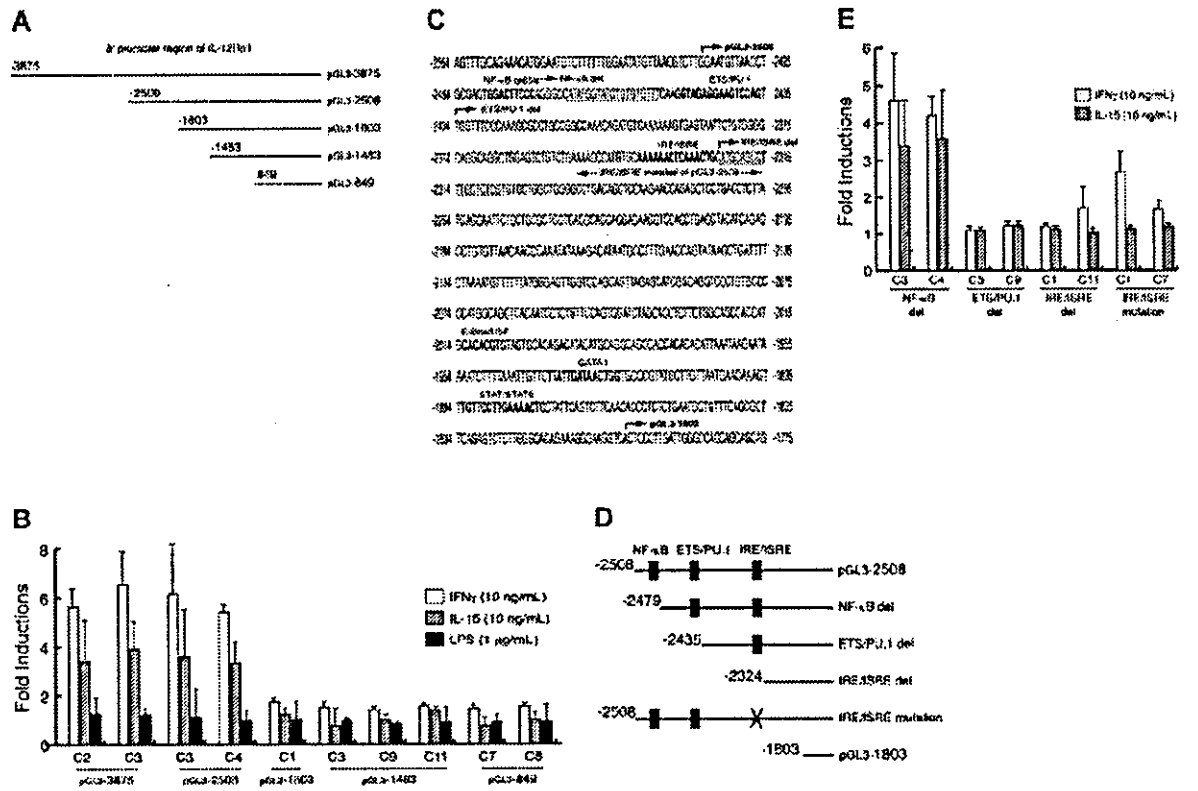


**Figure 2. Functional elements required for IL12RB1 transcriptional activation.** (A) Schematic presentation of the IL12RB1 promoter deletion constructs. A series of 5' promoter deletion constructs were cloned into pGL3-basic vector and were stably integrated into RAW264.7 cells. The number of each construct corresponds to its 5' end. (B) RAW264.7 cells stably integrated with IL12RB1 deletion constructs were cultured without serum at $1 \times 10^5$ cells/plate for 24 hours. Cells were left untreated or were treated with one of the following: 10 ng/mL IFN-γ, 10 ng/mL IL-15, or 1 μg/mL LPS for 8 hours before lysate preparation for luciferase assays. Luciferase activity from 2 independent clones of each deletion construct was examined. Basal luciferase activity of untreated cells was generally similar among all the examined clones. Results are expressed as fold induction over untreated controls (mean ± SD). (C) The nucleotide sequence of the region required for the IL12RB1 promoter activation by IFN-γ and IL-15, potential binding sites for transcription factors, are indicated by bold capital letters. Arrows identify the 5' end of deletion constructs, and nucleotides used as primers for ChIP assays were underlined. (D) Schematic presentation of the second series of IL12RB1 promoter deletion mutant. Black boxes represent binding elements for indicated transcription factors. (E) RAW264.7 cells stably integrated with a second series of promoter deletion mutant (as in panel D) were cultured and plated as described in panel B. Cells were left untreated or were treated with 10 ng/mL IFN-γ or 10 ng/mL IL-15 for 8 hours before lysate preparation and luciferase assays. Basal luciferase activity of untreated cells was generally similar among the examined clones. Fold inductions by IFN-γ or IL-15 are expressed as described in panel B.

IL-15, suggesting the region between −2508 and −1803 is essential for transcriptional induction. In contrast, neither of these constructs showed inducible promoter activity in response to LPS (Figure 2B).

Nucleotide analysis of the −2508 to approximately the −1803 region revealed binding sites for NF-κB, ETS/PU.1, IRE/ISRE, E-Box/USF, GATA1, and STAT/STAT5 (Figure 2C). We thus generated the second series of promoter deletion constructs, which specifically deleted NF-κB, ETS/PU.1, or IRE/ISRE (Figure 2D). As shown in Figure 2E, IL12RB1 promoter activation by IFN-γ or IL-15 was not affected by the removal of the NF-κB consensus element. In contrast, deletion of ETS/PU.1 (ETS/PU.1 del) abolished IL12RB1 promoter activation by IFN-γ or IL-15. To further examine the involvement of the IRE/ISRE binding site, the IRE/ISRE sequence of pGL3-2508 was independently mutated (IRE/ISRE mutation). The IRE/ISRE mutation significantly inhibited, but did not abolish, promoter activation by IFN-γ, whereas it completely abrogated the responsiveness to IL-15. Taken together, ETS/PU.1 and IRE/ISRE, but not NF-κB consensus elements, seemed essentially involved in IL12RB1 transcriptional activation by IFN-γ and IL-15.

### Protein binding to the ETS/PU.1 and IRE/ISRE consensus elements in the IL12RB1 promoter

We next examined the protein-DNA binding responsible for IL12RB1 gene activation using EMSA. Nuclear extracts prepared from untreated, IFN-γ–, IL-15–, or LPS-treated RAW264.7 cells were incubated with $^{32}$P-labeled double-strand oligonucleotides corresponding to the NF-κB, ETS/PU.1, IRE/ISRE, E-Box/USF, GATA1, or STAT/STAT5 consensus binding site of the IL12RB1 promoter (Figure 3A-B). EMSA revealed that stimulation with IFN-γ or IL-15 potently induced protein binding to ETS/PU.1 and IRE/ISRE consensus elements but not to NF-κB, E-Box/USF, GATA1, or STAT/STAT5 elements. The protein binding complexes of ETS/PU.1 and IRE/ISRE were specific because they were abrogated by the addition of excess unlabeled specific oligonucleotides.

To further identify protein binding to the IRE/ISRE consensus element, we used 5- or 50-fold excesses of unlabeled, synthetic, double-strand oligonucleotides that specifically bind to interferon regulatory factor 1 and 2 (IRF1/2), IRF3, IRF7, and IRF3/7 transcription factors or to a mutated form of IRF3/7 consensus sequence to block the IRE/ISRE–protein complex formation.[28] As